Ultra-sensitive isotope probing to quantify activity and substrate assimilation in microbiomes

Authors:

Manuel Kleiner[1#], Angela Kouris[2], Marlene Jensen[1], Grace D'Angelo[1,3], Yihua Liu[2,4], Abigail Korenek[1], Nikola Tolić[5], Timo Sachsenberg[6], Janine McCalder[2], Mary S. Lipton[5], and Marc Strous[2#]

[1]Department of Plant and Microbial Biology, North Carolina State University, Raleigh, North Carolina, USA

[2]Department of Geoscience, University of Calgary, Calgary, Alberta, Canada

3Max Planck Institute for Marine Microbiology, Bremen, Germany

4Max Planck Institute for Biology, Tübingen, Germany

5Environmental Molecular Science Laboratory, Pacific Northwest National Laboratory, Richland, Washington, USA

6Institute for Bioinformatics and Medical Informatics, University of Tübingen, Tübingen, Germany

#corresponding authors

Manuel Kleiner: manuel_kleiner (AT) ncsu.edu

Marc Strous: mstrous (AT) ucalgary.ca

Abstract

Stable isotope probing (SIP) approaches are a critical tool in microbiome research to determine associations between species and substrates. The application of these approaches ranges from studying microbial communities important for global biogeochemical cycling to host-microbiota interactions in the intestinal tract. Current SIP approaches, such as DNA-SIP or nanoSIMS, are limited in terms of sensitivity, resolution or throughput. Here we present an ultra-sensitive, high-throughput protein-based stable isotope probing approach (Protein-SIP), which cuts cost for labeled substrates by ~90% as compared to other SIP and Protein-SIP approaches and thus enables isotope labeling experiments on much larger scales and with higher replication. It allows for the determination of isotope incorporation into microbiome members with species level resolution using standard metaproteomics LC-MS/MS measurements. The analysis has been implemented as an open-source application (https://sourceforge.net/projects/calis-p/). We demonstrate sensitivity, precision and accuracy using bacterial cultures and mock communities with different labeling schemes. Furthermore, we benchmark our approach against two existing Protein-SIP approaches and show that in the low labeling range used our approach is the most sensitive and accurate. Finally, we measure translational activity using 18O heavy water labeling in a 63-species community derived from human fecal samples grown on media simulating two different diets. Activity could be quantified on average for 27 species per sample, with 9 species showing significantly higher activity on a high protein diet, as compared to a high fiber diet. Surprisingly, among the species with increased activity on high protein were several *Bacteroides* species known as fiber consumers. Apparently, protein supply is a critical consideration when assessing growth of intestinal microbes on fiber, including fiber based prebiotics. In summary, we demonstrate that our Protein-SIP approach allows for the ultra-sensitive (0.01% to 10% label) detection of stable isotopes of elements found in proteins, using standard metaproteomics data.

52 # Introduction

53 Microbial communities drive chemical transformations from global element cycling to human
54 nutrition. Unfortunately, the overwhelming complexity of these communities is often a barrier to
55 unraveling their functionality. Use of isotopic or chemical labeling is a powerful solution to that
56 problem. Even in the context of complex microbial communities, labeling enables assigning
57 activities and functions to taxa, tracking metabolic pathways and resolving trophic relationships
58 among species[1–5]. Current labeling approaches include use of click-chemistry (BONCAT)[6],
59 nanoscale secondary ion mass spectrometry (nanoSIMS)[2], Raman microscopy [7], genomic
60 sequencing of isotope labeled DNA/RNA (DNA/RNA-SIP)[8], separated from unlabeled
61 DNA/RNA with density gradient centrifugation, and protein-based stable isotope probing
62 metaproteomics (Protein-SIP)[9]. Some of these approaches use labels with defined chemistry
63 such as non-canonical amino acids in BONCAT[6], which are directly assimilated into biomass.
64 Others use more generic labels, such as substrate molecules labeled with heavy isotopes of
65 carbon, nitrogen, oxygen and hydrogen[2,7,10,11]. When spatial organization of samples is
66 important, approaches are available to image labeling outcomes[12,13]. When it is unknown in
67 advance which species or pathway might be involved in a target process, labeling can be
68 combined with untargeted metagenomics and metaproteomics analyses.

69 Recently, we developed an algorithm (Calis-p 1.0) to estimate natural isotope abundances
70 (stable isotope fingerprints, SIF) of carbon isotopes of individual species within complex
71 microbial communities using metaproteomics [14]. In nature, ^{13}C and ^{12}C occur side by side at a
72 ratio of approximately 0.011 $^{13}C/^{12}C$. For microbial biomass, very subtle changes to this ratio, as
73 little as 0.0001, already provide information about carbon assimilation pathways and carbon
74 sources used. Our algorithm, which modeled mass spectra of individual peptides using Fast
75 Fourier Transformations (FFTs), was able to detect these subtle changes. In the present paper we
76 further develop this extremely sensitive approach to also work for stable isotope probing (SIP)
77 experiments. This enables us to detect and quantify the assimilation of heavy isotopes by
78 individual species in complex microbial communities using metaproteomics (Protein-SIP).

79 Protein-SIP differs from other metabolic labeling approaches in that the heavy isotopes
80 from the substrate are incorporated into protein through *de novo* synthesis of amino acids from
81 the substrates via biosynthetic pathways, rather than directly in the form of labeled amino acids.
82 Such labeled amino acids are used, for example, in the "Stable Isotope Labeling by Amino Acids
83 in Cell Culture" (SILAC) approach [15]. The "random" incorporation of label into various amino
84 acids and ultimately into peptides makes data analysis much more complicated in Protein-SIP, at
85 least compared to the predictable exact mass shifts resulting from direct assimilation of labeled
86 amino acids in SILAC.

87 Protein-SIP approaches have been successfully developed before, but these approaches
88 have their challenges (for an overview see introduction of [10]). Metaproteomics relies on high-

resolution mass spectrometry to detect, identify and quantify peptides, which are then used for protein identification and quantification[16]. Using the same mass spectra already used for peptide identification to also quantify abundances of heavy isotopes in these peptides appears a straightforward add-on, as these spectra resolve the peptide isotopes and provide their intensities. However, unknown amounts of heavy isotopes shift peptide mass peaks by unknown numbers of mass-units, which makes the identification of peptides based on masses computationally challenging. The existing Sipros algorithm solved this problem with brute force by coupling the detection of labeled peptides with the initial peptide identification. Sipros predicts the most abundant peptide masses and isotopic distributions of b and y ions in an isotope atom% range of 0 - 100% in 1% increments[17]. This approach makes Protein-SIP experiments computationally so expensive that dedicated smaller protein sequence databases have to be constructed for determination of stable isotope content of peptides[18] and even then the approach still requires a supercomputer to work. For example, one study using the Sipros approach had to invest around 500,000 CPU hours for a study with less than 10 labeled samples[10]. The MetaProSIP[19] and SIPPER [20] algorithms overcame the problem by using spectra of unlabeled peptides as a starting point for computations. In case of MetaProSIP these unlabeled peptides can be derived from the SIP experiment itself if a portion of the original unlabeled proteins is still present, or, alternatively, from a control sample that was incubated without label. MetaProSIP then detects the labeled peptides corresponding to the unlabeled peptides and computes the relative isotope abundance and labeling ratio based on the comparison of the labeled and unlabeled form of peptides [19]. Because MetaProSIP requires a labeled peptide's spectrum to be shifted away from the mono-isotopic mass, it has been speculated that it requires relatively heavy labeling (e.g. >20.24 atom% for ^{13}C and >73.1 atom% for ^{15}N [21]). In case of SIPPER the isotopic patterns for unlabeled peptides are generated in silico and subtracted from the experimental isotope patterns of peptides. Remaining peak intensities after subtraction are used for estimating isotope content. SIPPER is designed to detect small changes in isotopic profiles of complex mixtures after short exposure to 13C label, with proposed scoring schemes to reduce the rate of false discoveries.

While the identification challenges can be solved by clever algorithms, underneath these challenges hides a more fundamental problem. Figure 1 shows the expected mass spectra of three *E. coli* peptides after 1/8 generation of labeling with ^{13}C-glucose. The figure illustrates the problem with these data: Assimilation of heavy isotopes into peptides leads to broadening of spectra. Thus, a peptide's matter gets divided over ever more peaks, reducing sensitivity. Also, because many peptides get injected into the mass spectrometer simultaneously, especially for complex samples such as a microbial community, the probability of the peptide's spectrum overlapping with another spectrum increases as it broadens, reducing data quality. Heavy peptides are especially sensitive to these issues. Counter-intuitively, for Protein-SIP, sensitivity is highest when using small amounts of label.

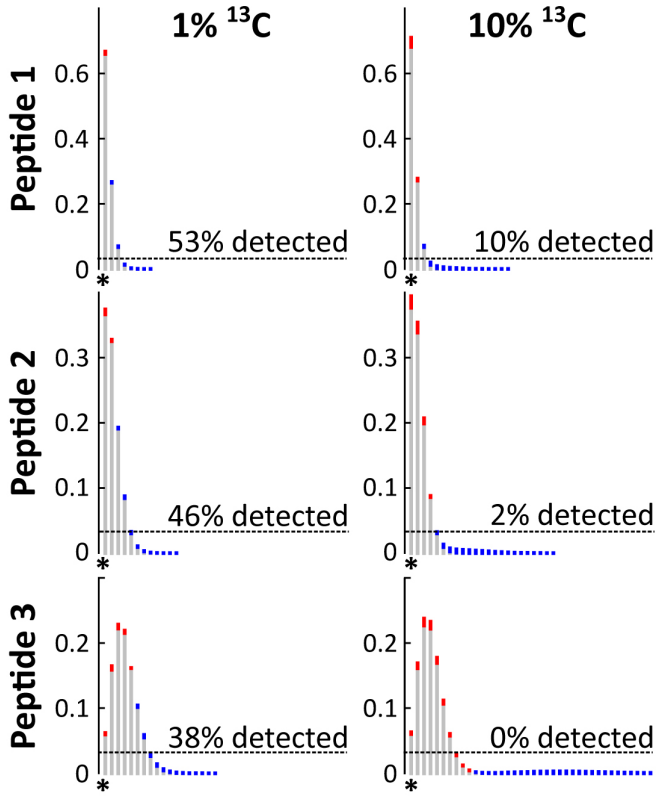

Figure 1: Modeled spectra of three *E. coli* peptides after ⅛ generations of growth on 1% (left) and 10% (right) $^{13}C_{1\text{-}6}$ glucose (13C/12C 0.02 and 0.11 respectively). Assimilation of 13C into peptides leads to a shift of matter away from from the monoisotopic mass (shown as *). The resulting peak intensity changes are shown in red - for peaks with decreased intensity -, and blue - for peaks with increased intensity after labeling. Dashed lines show experimentally determined average detection limits for peaks (see methods). Peaks below the dashed line are not recorded by the mass spectrometer. Percentages above lines indicate how much of the actual change is detectable in practice. Peptide 1 - IGLETAR; peptide 2 - AFEMGWRPDMSGVK; peptide 3 - QIQEALQYANQAQVTKPQIQQTGEDITQDTLFLLGSEALESMIK.

Our previous algorithm was developed to estimate slight differences in isotopic content based on peptide mass spectra, to determine natural carbon isotope abundances[14]. It made use of the fact that in nature, heavy isotopes are distributed randomly, yielding spectra that are perfect Poisson distributions. This enabled us to reduce the noisiness of the data by identification and rejection of imperfect spectra. Spectra in Protein-SIP experiments do not have such conveniently predictable properties. With labeled samples, the shape of spectra cannot be predicted using FFT, because these spectra become mixtures of spectra associated with labeled and unlabeled peptides. Both the proportion of heavy isotopes in the labeled peptides and the extent of labeling - the relative abundances of labeled versus unlabeled populations of peptides - are unknown in advance. For analysis of these data we therefore developed rigorous noise filtering and estimated isotopic content based on neutron abundance, requiring no assumptions about a spectrum's shape.

We present new algorithms and software for sensitive and quantitative estimation of isotopic content of individual species in stable isotope probing experiments with complex microbial communities. The new algorithms have been integrated into the Calis-p software together with the SIF algorithms, and the software was completely re-written to enable Protein-SIP (new version is Calis-p 2.1). The software decouples peptide identification from label detection and is thus compatible with most standard peptide identification pipelines. Computation of label content is very fast, a high-end desktop computer only needs one minute for processing ~1 Gb of data, corresponding to ~10,000 MS1 spectra or ~40 min of Orbitrap runtime. Using pure cultures of bacteria and mock communities, we show that Protein-SIP with Calis-p yields best results when substrates are partially labeled. For example, for carbon the fraction of heavy atoms should make up <10% of the total. For abundant organisms, assimilation of label (such as ^{13}C) into protein can be quantified within minutes after adding the label, within 1/16 of a generation. Even for rare organisms making up ~1% of a community, a single generation of labeling is sufficient for robust detection of label assimilation. We believe these advances will be helpful to microbiome researchers and microbial ecologists seeking to assign functions and activities to taxa, to track metabolic pathways and for resolving trophic relationships among species.

Results

Previously we presented algorithms and software for estimating natural isotope fingerprints from peptide mass spectra[14]. Our previous algorithm made use of the stochastic distribution of isotopes in nature and mass spectra that can be modeled by Fast Fourier Transformations. Quality control is intrinsic to that approach, as poor quality spectra cannot be modeled with FFT and can be rejected. Examples of low quality spectra are spectra that overlap with other spectra or low intensity spectra that are affected by noise. Feeding microbes labeled substrates for Protein-SIP experiments leads to peptide mass spectra with irregular shapes that cannot be modelled with FFT, as explained in the introduction. Isotopic composition of such spectra can still be inferred, by adding up the mass intensities of all peaks in the spectrum according to Equation 1 in the Methods (implemented as “neutron abundance” model in Calis-p). Unfortunately, that approach does not enable rejection of low quality spectra. Therefore, we implemented a simple noise filter based on unsupervised Markov clustering of all spectra associated with a single peptide (see Materials and Methods for details). The assumption underlying this approach is that most spectra are relatively unaffected by noise and will form the largest cluster. Spectra outside the largest cluster should be rejected for being of lower quality.

The performance of this filter was benchmarked using previous natural-isotope abundance data of pure cultures and mock communities of microbes (Suppl. Results & Discussion, Fig. S1, Tables S1 & S2). The FFT estimates of $^{13}C/^{12}C$ ratios for filtered spectra was as good or better than reported previously without filtering[14]. Even better, after filtering the estimates of $^{13}C/^{12}C$

184 ratios according to Equation 1 (see Materials and Methods) were now almost as good as for FFT.
185 The average difference between the actual and estimated median $\delta^{13}C$ values for the fifteen most
186 abundant organisms of a mock community was 2‰ for FFT and 4‰ for the neutron abundance
187 model. Implementation of the filter also dramatically reduced computation times because fewer
188 FFT operations were needed.

189 To test the performance of Equation 1 for ^{13}C labeled peptides, we labeled cells of two
190 model organisms, *Escherichia coli* K12 and *Bacillus subtilis* ATCC 6051, to saturation, with ^{13}C
191 glucose. Three replicate cultures were grown overnight with fully-labeled glucose ($^{13}C_{1-6}$) and
192 single-labeled glucose ($^{13}C_2$), with the percentage spiked-in ^{13}C increasing from 0 and 10% of
193 total glucose in seven steps. The glucose that was used as unlabeled glucose had the natural ^{13}C
194 content of around 1.1%. Protein was extracted, peptides were prepared, subjected to LC-MS/MS,
195 and identified with SEQUEST HT in Proteome Discoverer and results analyzed in Calis-p (see
196 Materials and Methods).

197 Surprisingly, adding as little as 1% label could already severely compromise the identification of
198 peptides by search algorithms such as SEQUEST. For example, for *B. subtilis* average peptide-
199 spectrum matches (PSMs) dropped by almost 90% at 10% added label. To mitigate these losses,
200 we tested five potential improvements to search strategies (see Materials and Methods and
201 Supplementary Results & Discussion for details). These ranged from computationally costly,
202 open mass window searches to more confined, faster approaches. All strategies improved
203 identification outcomes (Fig. 2 & S2). However, for the "open search" and "dynamic
204 modifications" strategy, computation times became impractical. For example, basic peptide
205 identification on a high performance desktop computer with the SEQUEST algorithm for single
206 140 min LC-MS/MS file from a microbial community took 17 min to search with our standard
207 search parameters, while it took 72 min with a search strategy that included modifications of the
208 peptide termini, and 1,947 min for a search strategy with a open (20 Da) mass window. We
209 selected the Modifications of Termini (N=low, C=high) strategy as a practical compromise
210 between peptides identified and extra computation time needed. This strategy adds six custom
211 "post-translational" modifications to the protein identification search. These modifications
212 generated more PSMs by enabling addition of one to three neutron masses at the N-terminus of a
213 peptide and four to six neutron masses to its C-terminus. We observed a strong difference in how
214 label amount impacted the number of PSMs between B. subtilis and E. coli. For B. subtilis a
215 small amount of added label strongly increased the number of PSMs, which then sharply
216 dropped at 1% label. We currently have no good explanation for this phenomenon.

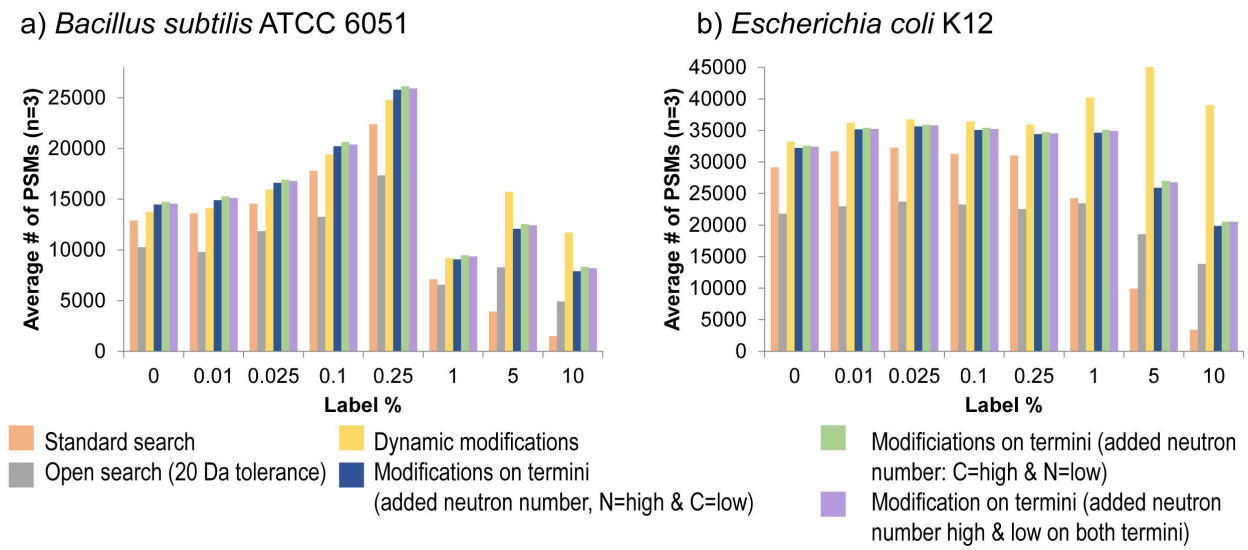

Figure 2: A small modification of the peptide identification approach drastically increases the number of peptides with 1-10% label that can be identified. Number of peptide spectral matches (PSMs) identified at different ^{13}C label percentages using six different peptide identification strategies. Cultures of a) *B. subtilis* and b) *E. coli* were grown in Bacillus minimal medium or M9 minimal medium (*E. coli*) in which a percentage of the glucose was replaced with $^{13}C_{1-6}$ glucose for >10 generations to achieve close to complete labeling. Three biological replicates were run for each label percentage. Peptides were identified using the SEQUEST HT Node in Proteome Discoverer (version 2.2) with six different strategies to account for the mass shifts caused by addition of heavy atoms. Standard search: no dynamic modifications to account for addition of label; Open search: the precursor mass tolerance was set to 20 Da allowing for the potential addition of 20 neutrons (e.g. ^{13}C atoms) in a peptide; Dynamic modifications: allowing for up to three dynamic modifications each of two custom peptide modifications adding a 1 neutron mass shift and a 2 neutron mass shift (up to 9 neutrons in total per peptide); Modifications on termini: six dynamic modifications were set up that were restricted to either the C or the N-terminus of the peptide. The modifications account for mass shifts of 1 to 6 neutrons and depending on the search strategy the low mass shifts (1, 2 and 3 neutrons) were set up as modifications on the C or the N-Terminus or low and high mass shift modifications were distributed between both termini. Each modification can only be added to a terminus once. This strategy allows for a total of 21 neutron additions to a peptide.

After assigning peptides to spectra with the improved peptide identification strategy, low quality spectra were rejected using the filter described above. For the remaining spectra, the number of neutron masses added as custom modifications during the identification step already provided a qualitative, or at best semi-quantitative, measure for label incorporation (Fig. 3, Suppl. Table S3). However, inference of the $^{13}C/^{12}C$ ratios by Equation 1 was much more precise, even for minimally (0.01%) labeled cells providing a limit of detection <0.01% label in most cases (see supplementary text). Precision and especially label recovery were both higher when using glucose labeled at only a single position rather than with fully labeled glucose. For the latter, the recovery was only 75-79%, meaning that the $^{13}C/^{12}C$ ratio was 21-25% lower than expected. Potentially, this was caused by broadening of spectra with fully labeled glucose (Fig. 1). As explained in the introduction, broader spectra reduce sensitivity. Interestingly, the breadth of spectra could be used to infer to what degree ^{13}C carbon was assimilated in clumps of multiple atoms (pie charts in Fig. 3). This approach, which only works when all atoms in a substrate are

249 labeled and when cells are labeled to saturation, could be used to infer the number of carbon
250 atoms in substrates that a given species is assimilating. In other words, Protein-SIP can provide
251 hints on whether a species is autotrophic or heterotrophic. We carried our similar labeling to
252 saturation experiments with 15N (E. coli labeled to saturation with 2.5% 15N ammonium) and
253 obtained similar results (data not shown, but available via PRIDE see data accessibility
254 statement).

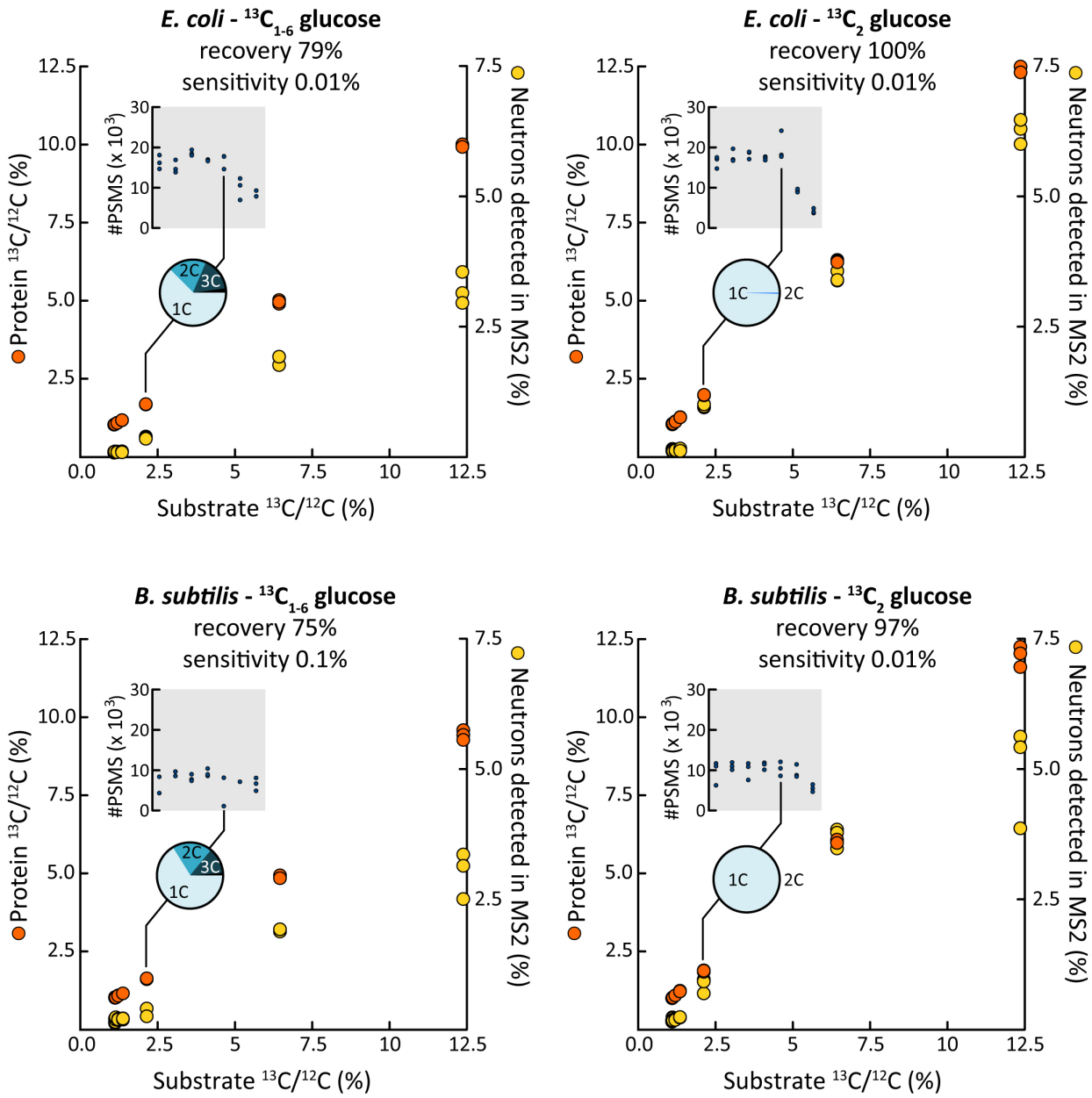

255

256 **Figure 3: The number of labeled atoms per substrate molecule impacts the ability to quantify label**
257 **incorporation accurately.** Labeling, to saturation, of *E. coli* and *B. subtilis* with single-labeled ($^{13}C_2$) and
258 fully labeled ($^{13}C_{1-6}$) glucose. The $^{13}C/^{12}C$ ratio in the substrate was varied. Note that unlabeled glucose
259 (0% added ^{13}C glucose) has a natural ^{13}C content of around 1.1%. Each orange circle is the median

260 $^{13}C/^{12}C$ ratio of all peptides measured in one replicate incubation (on average 2758 peptides per
261 replicate). Determined 13C/12C ratios increased linearly with substate $^{13}C/^{12}C$ ratios (R^2 >0.999). Almost
262 100% of the substrate ^{13}C was recovered in protein for $^{13}C_2$ glucose labeled cells. Recovery was lower for
263 $^{13}C_{1-6}$ glucose. The proportion of neutron masses detected via the improved peptide identification strategy
264 using N- and C-terminal modifications (yellow circles) increased with substrate $^{13}C/^{12}C$ ratios, but at low
265 linearity and sensitivity. The number of Calis-p filtered Peptide Spectrum Matches (PSM) decreased for
266 $^{13}C/^{12}C$ ratios above 2.5% (insets) as expected based on Figures 2 & S2. Assimilation of carbon into
267 amino acids in clumps of multiple ^{13}C atoms was detectable in peptide spectra of cultures fed with $^{13}C_{1-6}$
268 glucose as shown in pie charts for experiments fed with $^{13}C/^{12}C$ 1% above natural background. The
269 detailed data for this figure can be found in Suppl. Table S3.

270 The data of Figure 3 are not yet a meaningful representation of what an actual Protein-
271 SIP experiment would look like. In practice, we would always avoid labeling a microbial
272 community to saturation, because all community members would end up being labeled equally,
273 providing no new information on elemental fluxes and substrate uptake in the community. To
274 mimic an actual Protein-SIP experiment, we mixed labeled and unlabeled cells of *E. coli* at
275 different ratios, leading to compound spectra as shown in Figure 1.

276 The results indicated that estimation of $^{13}C/^{12}C$ ratios with this type of compound spectra was
277 more challenging (Fig. S3, Suppl. Table S4). Also, the difference between single labeled and
278 fully labeled glucose was more pronounced, with the former yielding much better sensitivity and
279 label recovery than the latter. For example, at 1% label recovery was 92% for single labeled
280 glucose, while it was 80% for glucose with 6 labeled carbons.We also compared the performance
281 of two center statistics for $^{13}C/^{12}C$ ratios, the intensity-weighted mean and the median. The
282 intensity-weighted mean displayed higher sensitivity and precision than the median in these
283 experiments (for contrasting results for community samples see below). However, both with 1%
284 and 10% single labeled glucose, even the median $^{13}C/^{12}C$ ratios accurately quantified label
285 assimilation within 1/16 of a generation (simulated by mixing of labeled and unlabeled cells),
286 corresponding to as little as 1-2 min of growth for *E. coli*.

287 Next, we investigated whether our approach was capable of detecting label assimilation
288 in the context of a microbial community. For this, we used a previously described mock
289 community, comprising >30 microbes, including gr+ and gr- bacteria, an archaeum, a eukaryote
290 (algae) and several phages[22]. This community also included *E. coli* K12, at ~6% abundance.
291 Here, we mixed cells of *E. coli* labeled with 1%, 5% and 10% $^{13}C_{1-6}$-glucose into the unlabeled
292 mock community at a ratio corresponding to one generation of growth for *E. coli*. Quantification
293 of ^{13}C assimilation was straightforward and linear (R^2 0.99, Fig. 4A, Suppl. Table S5). This was
294 perhaps not surprising because a relatively large amount of label was used and the relative
295 abundance of *E. coli* in the mock community was high, i.e. ~12% after addition of the labeled
296 cells.

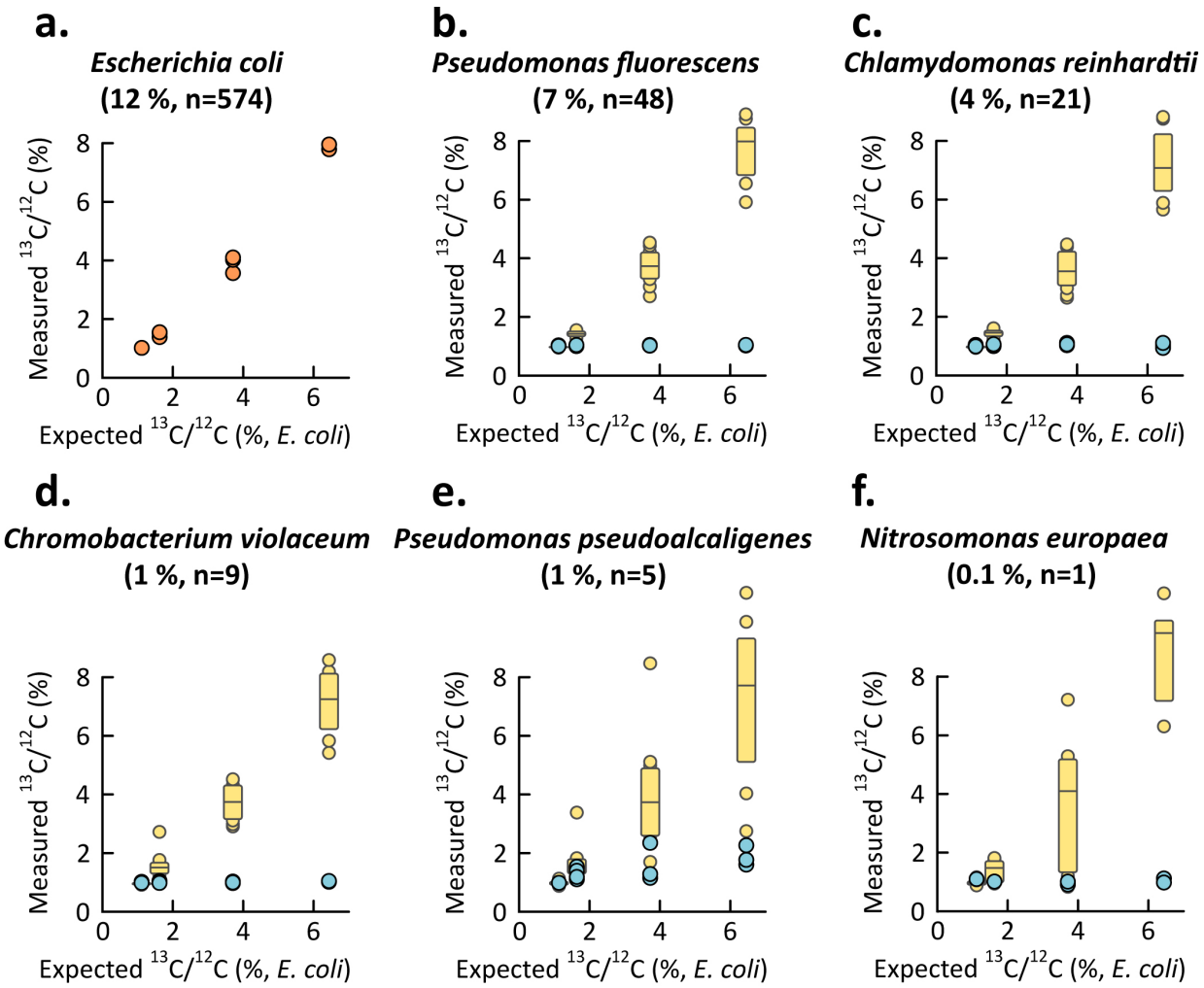

Figure 4. Detection of ^{13}C assimilation by *E. coli* within a mock community of 32 microorganisms developed by [22]. In each experiment, half of the *E. coli* cells were labeled using $^{13}C_{1\text{-}6}$-Glucose, corresponding to one generation of labeling, with glucose containing 0, 1, 5, and 10% ^{13}C on top of natural abundance ^{13}C (three replicate samples were generated for each labeling percentage and measured separately). Label incorporation by *E. coli* (**orange circles in a**), but not by other organisms (**blue circles shown for five organisms in b-e**), was clearly detectable and reproducible. Yellow box plots show the measured ^{13}C content of sets of *E.coli* peptides, obtained by downsampling of the results in **a**, mimicking the spectral intensities of the peptides collected for each unlabeled organism in panels **b-e** i.e. only *E. coli* peptides that corresponded in intensity to peptides of the analyzed organism were used. The percentage in parentheses indicates the relative abundance of the organism in the mock community based on its proteinaceous biomass and the "n=" indicates the average number of peptides passing the filters in Calis-p for SIP value calculation for the organism in each experiment, which also corresponds to the number of *E. coli* peptides used in downsampling. These results show label incorporation can be estimated, even for relatively rare species. Suppl. table S5 shows results for each species.

Figure 4 also shows to what extent the addition of the labeled cells of *E. coli* led to the incorrect inference of label assimilation by five other members of the mock community. The relative abundance of these unlabeled organisms was between 0.1% and 7% . The determined $^{13}C/^{12}C$ ratios for the >20 other members of the mock community are reported in supplementary table S5. We found that the choice of center statistic used has a major impact on the false

317 positive detection of label incorporation. When using the median, the overall (i.e. all unlabeled
318 species in all replicates) False Positive Rate (FPR) of label detection for populations with nine or
319 more peptides (after filtering) was 3.4% and for populations with eight or fewer peptides it was
320 45%. In contrast, when using the weighted mean the FPR was 51% for populations with nine or
321 more peptides and 50% for populations with eight or less peptides. In our dataset, the nine
322 peptide threshold corresponded to ~1% relative abundance of strains/species within the mock
323 community. We investigated the massive differences in FPRs between the two center statistics
324 by manually checking spectra causing false positives and found that low-intensity peptide
325 spectra associated with less abundant populations were often affected by the overlap with
326 broadened spectra of a labeled, more-abundant population. Therefore, we concluded that for
327 label detection in microbial communities the median should be used (see detailed discussion in
328 supplementary methods). Figure 4 shows examples of false-positive inferences for
329 *Pseudomonas pseudoalkaligenes*.

330 To investigate whether label assimilation can be correctly inferred for less abundant
331 populations, we downsampled (bootstrapped, up to ten times) the set of >6,000 peptides
332 collected for *E. coli*, using the peptides of each other organism as templates. In the resulting
333 datasets, each *E. coli* peptide was matched to a peptide of the other organism with a similar
334 intensity. Based on inferences for these bootstrapped datasets shown in Figure 4, label
335 assimilation could be robustly estimated, at least for populations associated with nine or more
336 peptides, corresponding to ~1% abundance. This number of peptides is much smaller than the
337 ~30 peptides needed for estimation of natural carbon isotope content in a species using Protein-
338 SIF (Suppl. Results & Discussion, Fig. S1).

339 Next, we analyzed how well we could detect incorporation of label into individual
340 proteins based on how many peptides passed the Calis-p quality filters for a protein. For this we
341 analyzed the Calis-p reported $^{13}C/^{12}C$ ratios for proteins from the mock communities with 5%
342 labeled *E. coli* spiked-in and without spiked in *E. coli*. $^{13}C/^{12}C$ ratios in *E. coli* proteins from the
343 5% spike-in samples were on average much higher than the ratios for proteins from the unlabeled
344 mock communities and the unlabeled mock community members in the 5% spike-in samples
345 (Fig. 5a). Even for proteins for which only 1 peptide passed the Calis-p quality filters, this
346 pattern was observed. This indicated that label incorporation into individual proteins can be
347 detected with as few as 1 peptide. For some proteins from unlabeled organisms, for which 3 or
348 less peptides passed the Calis-p quality filter, $^{13}C/^{12}C$ ratios that were above the expected value
349 of 0.011 (Fig. 5a), indicating that, as expected, the accuracy of the ratio estimates increases with
350 more peptides available per protein.

351 To test if meaningful results can be obtained from populations in mixed communities that shift
352 their metabolism and physiology we analyzed $^{13}C/^{12}C$ ratios in *E. coli* proteins from the 5%
353 spike-in samples in more detail. For this analysis it is important to know that the unlabeled *E.*
354 *coli* cells that were part of the mock community were grown at well oxygenated conditions in a

355 complex medium containing organic nutrients such as amino acids and vitamins (LB broth),
356 while the *E. coli* grown in the presence of $^{13}C_{1-6}$-glucose (5% of total glucose) were grown under
357 oxygen limited conditions in a minimal medium (M9 broth) that contained glucose as the only
358 carbon source and nitrogen only in inorganic form. This mixing of unlabeled LB grown and
359 labeled M9 grown *E. coli* led to the following expectations: 1) proteins that are produced
360 exclusively or almost exclusively by cells growing on LB would show no label incorporation in
361 the 5% label mock communities and thus have $^{13}C/^{12}C$ ratios close to the expected value of
362 0.011; and 2) conversely proteins that are produced exclusively or almost exclusively by cells
363 growing on M9 would show high label incorporation in the 5% label mock communities ($^{13}C/^{12}C$
364 ratios of >0.04). We only looked at proteins that were detected in at least two replicates of one
365 condition (Suppl. Table S6, Fig. 5b). Proteins for the degradation of amino acids and other
366 carbon sources were unlabeled, indicating that they were only produced by *E. coli* in complex
367 medium, but not when growing on M9. Proteins for amino acid biosynthesis pathways,
368 glycolysis, mixed acid fermentation and iron acquisition were heavily labeled, indicating that
369 lack of amino acid sources in the medium led to expression of biosynthesis pathways, oxygen
370 limitation led to induction of fermentation pathways and that potentially cells growing in M9
371 were iron limited.

372

373

a) Detection of ^{13}C label in individual *E. coli* proteins of *E. coli* in a mock community

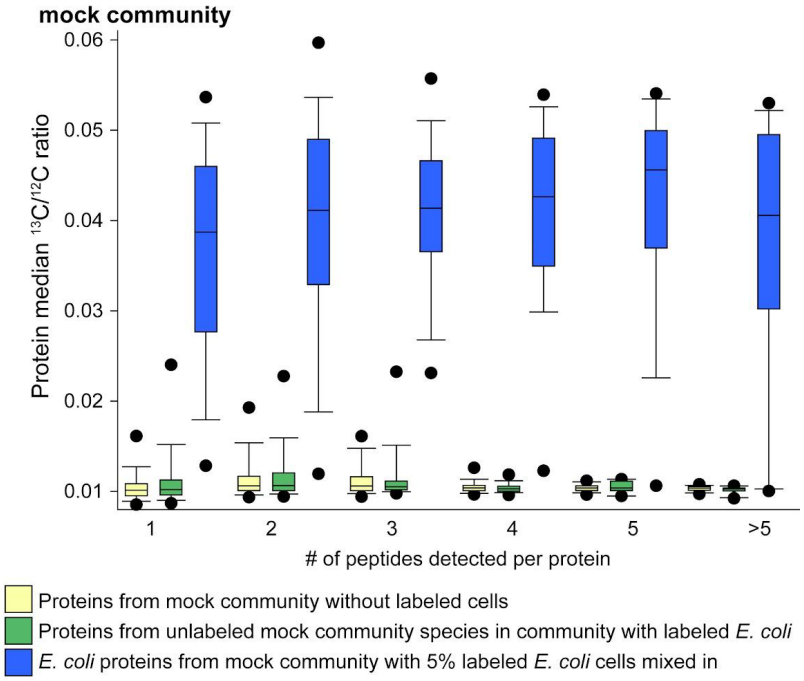

b) Examples of proteins from *E. coli* grown under different conditions with and without label and spiked into mock community

0%	5%	Accession	Annotation	General Pathway
0.010	ND	P00805	AnsB	Amino Acid Degrdadation
0.011	ND	P0A6T9	GcvH	Amino Acid Degrdadation
0.010	0.010	P0A853	TnaA	Amino Acid Degrdadation
0.010	0.011	P0AC38	AspA	Amino Acid Degrdadation
0.010	0.011	P0A6F3	GlpK	Glycerol Degradation
0.011	0.011	P69910	GadB	Amino Acid Degrdadation
0.012	0.012	P0AB77	Kbl	Amino Acid Degrdadation
0.010	0.013	P12758	Udp	Ribonucleoside degradation
0.011	0.013	P02925	RbsB	Ribose uptake
0.010	0.045	P0A6P9	Eno	Glycolysis
0.011	0.046	P0ADG7	GuaB	Ribonucleotide biosynthesis
0.011	0.046	P08839	PtsI	Sugar uptake (likely glucose)
0.010	0.047	P0AD61	PykF	Mixed Acid Fermentation
0.010	0.047	P06959	AceF	Glycolysis
0.011	0.049	P62707	GpmA	Glycolysis
0.011	0.051	P61889	Mdh	TCA, Mixed Acid Fermentation
0.011	0.051	P0ABK5	CysK	Amino Acid Biosynthesis
ND	0.045	P0A817	MetK	Amino Acid Biosynthesis
ND	0.045	P09832	GltD	Amino Acid Biosynthesis
ND	0.046	P0AB80	IlvE	Amino Acid Biosynthesis
ND	0.047	P23721	SerC	Amino Acid Biosynthesis
ND	0.047	P0A877	TrpA	Amino Acid Biosynthesis
ND	0.047	P00864	Ppc	Mixed Acid Fermentation
ND	0.047	P11454	EntF	Iron Acquisition
ND	0.048	P06987	HisB	Amino Acid Biosynthesis
ND	0.050	P00561	ThrA	Amino Acid Biosynthesis
ND	0.050	P0AEL6	FepB	Iron Acquisition
ND	0.051	P0ADI4	EntB	Iron Acquisition
ND	0.052	P0AB24	EfeO	Iron Acquisition
ND	0.053	P05825	FepA	Iron Acquisition

374

375 **Figure 5: Measurement of ^{13}C label content in individual proteins.** Analysis of a subset of the data
376 shown in Fig. 4. *E. coli* grown in standard LB medium without label (0% added label) was part of a mock
377 community consisting of 32 microorganisms [22]. To this mock community *E. coli* grown in minimal M9
378 medium with glucose (5% of total glucose as $^{13}C_{1-6}$-Glucose) in air tight bottles under oxygen limiting
379 conditions was added in a 1:1 ratio to the unlabeled LB grown *E. coli* cells in the mock community. **a)**
380 Detection of increased $^{13}C/^{12}C$ ratios in individual proteins as a function of the total number of different
381 peptides detected for each protein. Proteins from all species in the unlabeled mock community are
382 compared to the proteins of all unlabeled species in the mock community that contained the 5% labeled
383 *E. coli* cells, as well as to the proteins from *E. coli* in the mock community that contained the labeled *E.*
384 *coli* cells. The boxes indicate the 25th and 75th percentile, the line the median, the whiskers the 10th and
385 90th percentile, and the dots the 5th and 95th percentile. **b)** Examples of *E. coli* proteins that showed no
386 or high label incorporation in 5% ^{13}C glucose grown *E. coli* in the mock community. Unchanged $^{13}C/^{12}C$
387 ratios shown in the table between treatments indicate that proteins were not produced in cells that were
388 grown in M9 medium with labeled glucose, but were present in cells grown in LB. Proteins with high ratio
389 were mostly or exclusively produced by cells grown in M9. $^{13}C/^{12}C$ ratios in the table are averages of three
390 replicate samples. Only proteins that were detected in at least two replicates in one of the conditions are
391 shown. The full table is Suppl. Table S6.

392 **Comparison with existing Protein-SIP approaches**

393 To compare the performance of Calis-p with existing Protein-SIP approaches four of the above described
394 datasets with labeled E. coli spiked into a mock community were processed by expert operators of the
395 SIPPER and MetaProSIP workflows. We would like to highlight here that these two approaches were
396 developed for higher label amounts (MetaProSIP) and low level labeling after shot label exposure
397 (SIPPER) and they may well outperform Calis-p under specific conditions. However, we focused our
398 comparison on the low label amounts for which the ultra-sensitive Protein-SIP within Calis-p was
399 developed and a comparison at high label amounts (>10% label) was outside the scope of this study.

400 The three approaches differed strongly in the number of peptides for which label content was
401 quantified (Fig. 6b). Part of this was due to the fact that for each of the three approaches different peptide
402 identification algorithms were used (Fig. 6b) leading to differences in the number of peptides that served
403 as input for label quantification. The MSGF+ search engine used by SIPPER yielded the lowest number
404 of identified peptides. While MetaProSIP quantified label content for the highest proportion of input
405 peptides in all cases (>80%), Calis-p provided isotope contents for the lowest proportion of input peptides
406 (25-31%). This large difference for identified and isotopically quantified peptides for Calis-p is caused by
407 the multiple quality filtering steps in Calis-p that remove large numbers of peptides and spectra from
408 consideration for various quality related issues (e.g. flagged for No valid PSM' 'too few spectra' 'No
409 majority vote while clustering'). With the higher number of peptides for which 13C content was quantified
410 by MetaProSIP, MetaProSIP provided sufficient peptide numbers (>9 for a species) to quantify label
411 content for the highest number of species (Fig. 6, Fig. S4).

412 The three approaches also differed in the number of false positive detection of above natural
413 abundance 13C in peptides (Fig. S4, Tables S7 to S10) and species (Figs. 6a & S4). Calis-p
414 overestimated 13C content only in a small number of peptides and in none of the species (i.e. median
415 13C content was at or below expected value). MetaProSIP also did not overestimate label content in any
416 of the species, instead it had the tendency to underestimate isotope content of unlabeled species.
417 SIPPER had a high rate of false positive detections, while for the 1% labeled sample all 13C content
418 estimates (including the estimate for the labeled E. coli) were strongly underestimated. 13C content of
419 unlabeled species for which enough peptides were quantified (9 peptides) were strongly overestimated.
420 This false positive label detection is likely due to the underlying principle of SIPPER, which is to identify
421 labeled peptides, while not trying to classify unlabeled peptides. This means that truly unlabeled peptides

422 are not available for calculation of label content of species and a small number of false positive label
423 detection in peptides can lead to miss estimation of label content in species and proteins.

424 Finally, the three approaches also differed in the accuracy of 13C content estimates for the labeled E.
425 coli. For the 1% labeled E. coli Calis-p was the only approach to detect the label in E. coli with the median
426 13C content being close to the expected value (Figs. 6 & S4) indicating a higher sensitivity of Calis-p at
427 low label contents. For the 5% and 10% labeled E. coli all three approaches detected label in E. coli with
428 the median 13C values being closest to the expectation for Calis-p in both cases indicating a higher
429 accuracy of the Calis-p estimate.

430 In summary, while MetaProSIP outperformed Calis-p in terms of quantity of peptide isotope quantification,
431 Calis-p was more sensitive and accurate. The sensitivity of MetaProSIP was, however, much better
432 (detection down to at least 5% 13C) than recently suggested by Starke[21]. Both MetaProSIP and Calis-p
433 showed high specificity; the lower specificity shown by SIPPER was likely caused by SIPPER's primary
434 focus on the detection of labeled peptides. Finally, while all three tools are independent of the search
435 engine (in contrast to Sipros), Calis-p has been implemented to work with the open search engine output
436 format mzIdentML, which will minimize compatibility issues between search engine output and Calis-p.

a) Deviation of the median calculated SIP values from the expected value

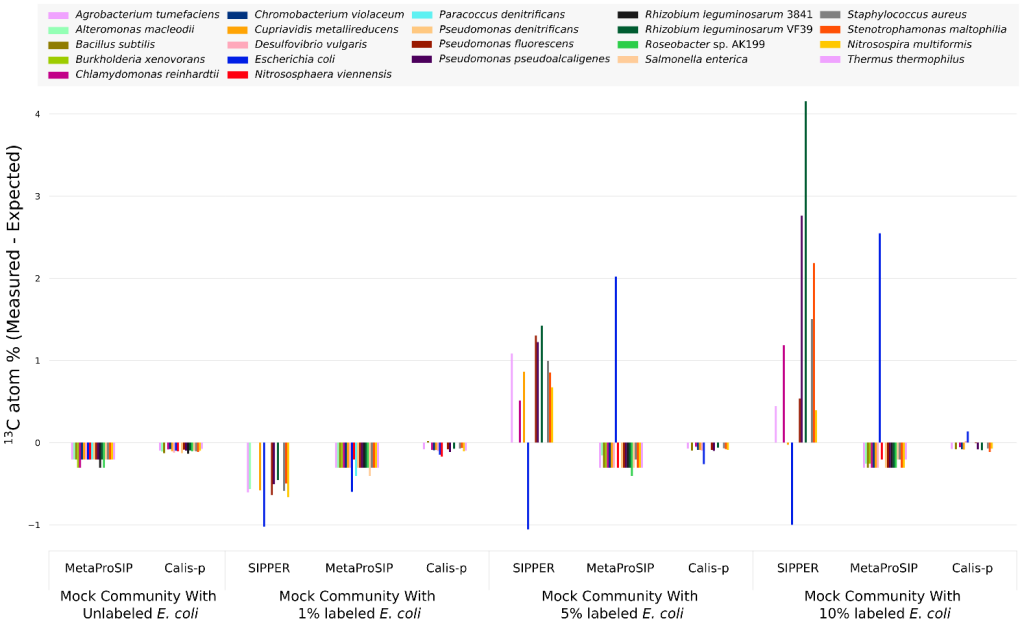

b) Total protein unique peptides identified and quantified with each SIP tool

Tool	Protein Unique Peptides (PUPs)	Dataset			
		Unlabeled *E. coli*	1% labeled *E. coli*	5% labeled *E. coli*	10% labeled *E. coli*
SIPPER	# PUPs* Identified	NA	10735	8226	5410
	# PUPs Isotopically Quantified	NA	4935	5227	3395
	% Quantified	NA	45.97	63.54	62.75
MetaProSIP	# PUPs Identified	22766	16264	10929	10187
	# PUPs Isotopically Quantified	19112	13053	8814	8325
	% Quantified	83.95	80.26	80.65	81.72
Calis-p	# PUPs Identified	27402	17266	13763	12208
	# PUPs Isotopically Quantified	6794	5389	3960	3223
	% Quantified	24.79	31.21	28.77	26.40

c) Overview of SIP tool parameters and filters used for comparison

	Identification Search Algorithm	Peptide FDR Cutoff	Database searching decoupled from SIP algorithm	Requires unlabeled reference sample	Compatible Heavy Isotopes	Extra Filtering of Output
SIPPER	MSGF+	5%	Yes	Yes	^{13}C	Distinct PUPs
MetaProSIP	comet	5%	Yes	No, increased sensitivity with unlabeled reference	^{13}C ^{15}N ^{18}O ^{2}H	Distinct PUPs, keeping highest relative isotope abundance per peptide
Calis-p	Sequest HT	5%	Yes	No	^{13}C ^{15}N ^{18}O	Distinct PUPs

Figure 6: Comparison of the output from the three Protein-SIP approaches: SIPPER, MetaProSIP, and Calis-p. Four datasets were processed by expert operators for each approach using optimal parameters for each approach. The outputs from each tool were filtered for comparability by retaining only distinct protein unique peptides (PUPs), defined as peptides unique to a protein sequence and with a unique combination of sequence, charge state, and m/z. a) Median 13C values were determined for organisms with 9 or more peptides. The expected 13C atom % value for each experimental condition was subtracted from each experimental SIP value and the deviation of the experimental value from the expected value is displayed. b) Table showing the total number of protein unique peptides identified and

446 used as the input for each approach and the total for which isotope values were quantified. c) Summary
447 of the parameters used for each tool/approach and additional post-processing steps as recommended by
448 each expert operator. Each tool output was filtered for distinct protein unique peptides i.e. isotope values
449 were only used if the peptide could be uniquely assigned to a single species. MetaProSIP required an
450 additional post-processing step for selecting the highest relative isotope abundance (RIA) value in cases
451 where the tool reported multiple RIA values. Detailed data for this figure is shown in Figure S4 and tables
452 S7 to S10.

453 Case Study: Differential heavy water incorporation reveals activity changes 454 for intestinal microbiota species in response to dietary changes

455 To demonstrate the power of the Calis-p approach and to test our approach for additional
456 elements we analyzed data from a complex microbial community grown with two types of heavy
457 water[11]. Both 2H and 18O water can function as markers of translational activity[10,23] and
458 thus allow to detect activity changes in members of microbial communities in response to
459 changes in environmental conditions or use of complex substrates without relying on direct
460 labeling with a specific substrate. The community consisted of 63 species isolated from human
461 fecal material and was grown in bioreactors with either a high fiber medium or a high protein
462 medium to simulate different dietary conditions encountered by the intestinal microbiota. For
463 each diet treatment three replicate cultures were grown for 12 hours with unlabeled water and
464 water in which 25% were either replaced with $^{2}H_{2}O$ or $H_{2}{}^{18}O$. We obtained thousands of
465 peptides passing Calis-p quality filtering for each sample (mean 4602 peptides/sample, SD 1140,
466 Fig. S5) and we were able to quantify heavy water incorporation (>9 peptides passing Calis-p
467 filters for species) for 21 to 30 species per sample (Mean = 27, Median = 28). We found that
468 overall incorporation of ^{18}O was much higher than incorporation of ^{2}H (Fig. S4). The low
469 measured incorporation of ^{2}H can potentially be attributed to variation in retention times of
470 isotopically different forms of a deuterated peptide in reversed-phase chromatography[24,25]. Such
471 retention time variation can generate distinct isotope patterns for the same peptide at different
472 retention times, which would lead to failure to cluster by the Markov clustering in Calis-p during
473 spectrum filtering. Since the amount of 2H used in this experiment was relatively high we do
474 expect relevant retention time shifts of deuterated peptides. Additional factors that might explain
475 low measured incorporation of ^{2}H are the known strong fractionation of hydrogen isotopes in
476 organisms[26], the fact that many hydrogen atoms on peptides can freely exchange with water
477 leading to loss of label during sample preparation[27], the dilution of 2H in stable C-H bonds in de
478 novo synthesized amino acids by hydrogens derived from organic growth substrates[23,28], and the
479 known toxicity of deuterium to many organisms slowing down their growth rates and thus
480 reducing the rate of incorporation, which however usually occurs at higher concentrations
481 (>50%) of deuterium than used in this experiment[23,29]. Finally, incorporation of ^{18}O over ^{2}H
482 may be favored because for incorporation of ^{18}O into non-exchangeable positions amino acid *de*
483 *novo* synthesis is not required. ^{18}O can be incorporated into the carboxyl group of amino acids
484 during proteolytic cleavage of substrate proteins[30] and remain in the peptide bond upon
485 formation of new peptide bonds. While ^{18}O in peptide bonds is stable and does not freely

exchange with water, ^{2}H in many positions on the peptide readily exchanges with H from water[27]. For hydrogen to be in positions with low exchangeability, amino acid *de novo* synthesis is required, because the necessary carbon-hydrogen bonds are only generated then[27].

On the whole community level, label incorporation was significantly higher in communities grown with high protein as compared to high fiber (Fig. S5**).** On the level of single species we observed that responses to a change in "diet" were species-specific with some species such as *Akkermansia muciniphila*, *Bacteroides ovatus*, and *Clostridium bolteae* incorporating significantly more label under high protein conditions, while other species, such as *Alistipes onderdonkii*, *Clostridium lavalense*, and *Flavonifractor plautii*, showed no change or non-significant trends towards higher incorporation under high fiber conditions (Fig. 7). While incorporation trends for species between ^{2}H and ^{18}O were mostly consistent with each other, much fewer comparisons tested significant for ^{2}H (4 for ^{2}H versus 9 for ^{18}O) likely due to the overall low measured incorporation of ^{2}H and resulting low sensitivity. Our results indicate that availability of higher amounts of protein increases the translational activity of many intestinal microbiota species, which is in line with previous studies showing nitrogen, and by extension protein, is the limiting nutrient for the intestinal microbiota[31,32]. This indicates that mixed community bioreactors can be a useful analog to the intestinal tract for studying specific ecological factors (such as nitrogen limitation) driving community function. Surprisingly, although typically described as fiber degrading specialists[33–35], we saw a significant increase of activity in several *Bacteroides* species in the high-protein medium relative to the high-fiber medium. This shows that it is critical to assess nitrogen/protein supply when analyzing fiber dependent growth of intestinal microbes. Furthermore, it suggests that nitrogen/protein supply is critical to consider when developing fiber based prebiotics to manipulate intestinal microbiota species[36,37], which to our knowledge has not been considered so far. In summary, our results show that the use of heavy water for Protein-SIP allowed us to detect changes in the activity of microbiota members in response to changes in complex substrates.

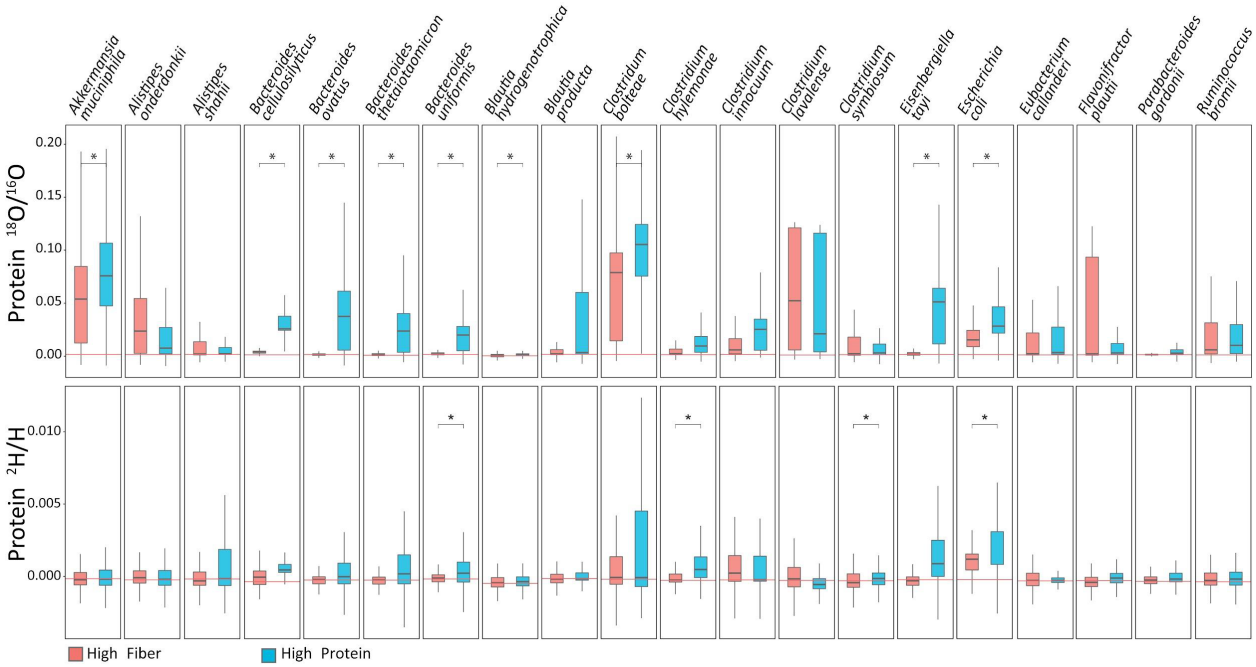

Figure 7: Strong differences in heavy water incorporation in intestinal microbiota species in response to diet. 63 species isolated from human intestinal microbiota were grown together in triplicates in either a high fiber or high protein medium in the presence of unlabeled water or water with either 25% ^{2}H or ^{18}O[11]. Calis-p based stable isotope ratios are shown for the 20 species for which at least 9 peptides passed Calis-p filtering conditions in all replicates. Each box shows the data for all peptides of the triplicate cultures combined (27 to 2225 peptides per box). The red lines indicate the average median for each species in the control samples with unlabeled water. Statistically significant differences are indicated with '*' based on Student's t-test on the means of replicates at $p<0.05$.

BOX: Summary of Practical Workflow Considerations

The Protein-SIP workflow consists of several steps including (1) incubation of a microbial community with a isotopically labeled substrate, (2) metaproteomic sample preparation and LC-MS/MS data acquisition, (3) peptide identification, (4) data conversion and input to Calis-p, (5) isotope pattern extraction and computation of isotope content in Calis-p, and (6) analysis and interpretation of data provided by Calis-p (Fig. 8). The provision of isotopically labeled substrates in experiments can take many forms, such as addition of substrate to incubations of enrichment cultures/bioreactors[11], addition to animal feed[38,39], CO_2 in plant incubation chambers[40] or as ^{15}N in plant fertilizer, and *in situ* incubations[10]. For the Protein-SIP approach presented here, substrate should be supplied with 1-10% of the total substrate containing the heavy isotope (label). Please note that this range refers to ^{13}C, for other elements, such as N, which make up a smaller portion of atoms in a peptide, a higher amount of label can be used, as the associated peptide mass shifts are smaller. If the substrate is a small molecule (e.g. glucose), but contains multiple atoms per molecule of the element to be labeled, ideally only one of the atoms is labeled (or a small portion of atoms if it is a very large molecule) to avoid isotope "clumping", as this can lead to a reduction in sensitivity (Fig. 3). Calis-p can,

537 however, handle "clumped" data if needed. Similarly, if a complex substrate is used (e.g.
538 complete plant leaves) ideally the complex substrate should only be partially labeled (e.g. by
539 growing plants in an atmosphere with 10% of the CO_2 being labeled) rather than using fully
540 labeled substrate.

541 Other considerations for the labeling experiments include the number of replicates that
542 are required, which depends on the biological question of the experiment, if a time course or a
543 single time point will be sampled, and if a control with unlabeled substrate will be carried out,
544 which is not needed for Calis-p, but can be helpful in data interpretation. Generally, we
545 recommend to carry out a feasibility study, if at all possible, to determine the correct amount of
546 label that works for the study system and time points that need to be sampled. Measurement of
547 bulk label incorporation using an isotope ratio mass spectrometer can be useful in determining if
548 an experiment worked prior to starting sample preparation for Protein-SIP.

549 The produced samples should be processed with a standard metaproteomic sample
550 preparation method tuned to the particular sample type. In contrast to the protein-SIF method [14],
551 which requires calibration for a small isotope offset caused by the instrument, no calibration
552 reference material needs to be prepared for Protein-SIP. The produced peptide mixtures need to
553 be analyzed by 1D or 2D liquid chromatography (LC) and tandem mass spectrometry (MS/MS)
554 using a high-resolution Orbitrap mass spectrometer with standard metaproteomic LC-MS/MS
555 approaches (see Methods and e.g. [41]). One important consideration for the data acquisition in
556 the mass spectrometer is the choice of resolution particularly for experiments involving ^{15}N
557 labeling (see Suppl. Results and Discussion).

558 The steps for data preparation for Calis-p and the computational steps implemented in
559 Calis-p are described in detail in the Methods and on the Calis-p software repository website
560 (https://sourceforge.net/projects/calis-p/).

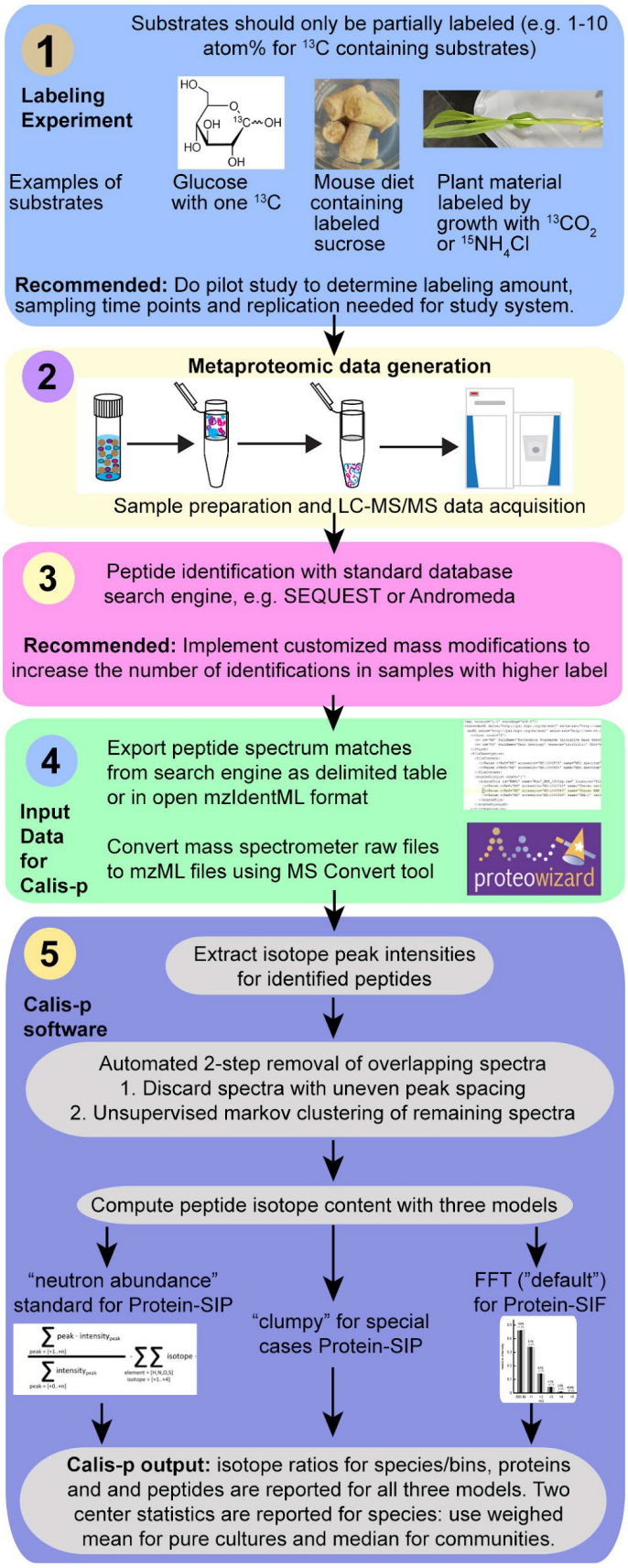
1
Substrates should only be partially labeled (e.g. 1-10 atom% for 13C containing substrates)
Labeling Experiment
Examples of substrates
Glucose with one 13C
Mouse diet containing labeled sucrose
Plant material labeled by growth with 13CO2 or 15NH4Cl
Recommended: Do pilot study to determine labeling amount, sampling time points and replication needed for study system.
2
Metaproteomic data generation
Sample preparation and LC-MS/MS data acquisition
3
Peptide identification with standard database search engine, e.g. SEQUEST or Andromeda
Recommended: Implement customized mass modifications to increase the number of identifications in samples with higher label
4
Input Data for Calis-p
Export peptide spectrum matches from search engine as delimited table or in open mzIdentML format
Convert mass spectrometer raw files to mzML files using MS Convert tool
proteowizard
5
Calis-p software
Extract isotope peak intensities for identified peptides
Automated 2-step removal of overlapping spectra
1. Discard spectra with uneven peak spacing
2. Unsupervised markov clustering of remaining spectra
Compute peptide isotope content with three models
"neutron abundance" standard for Protein-SIP
"clumpy" for special cases Protein-SIP
FFT ("default") for Protein-SIF
Calis-p output: isotope ratios for species/bins, proteins and and peptides are reported for all three models. Two center statistics are reported for species: use weighed mean for pure cultures and median for communities.

561

562 **Figure 8:** Protein-SIP and direct Protein-SIF workflow using Calis-p 2.1. The data filtering and
563 computations illustrated in step (5) all happen in Calis-p in a fully automated fashion. The user has the
564 ability to set specific parameters when starting the program. Full details on how to operate Calis-p are
565 provided in the Wiki at https://sourceforge.net/projects/calis-p/. Not shown in the figure is that for Protein-
566 SIF calibration of values with a reference material is needed, for details on this see the supplementary
567 text and the original Protein-SIF publication[14].

568 Discussion

569 The developed Protein-SIP approach provides a means to detect and quantify the incorporation
570 of stable isotopes from labeled substrates into many individual species in microbial communities
571 in one LC-MS/MS measurement and with minimal computational cost. Our approach has many
572 advantages over other SIP approaches and previously developed Protein-SIP approaches. First,
573 the approach allows for high throughput, as compared to most other stable isotope probing
574 methods, such as DNA/RNA-SIP and nanoSIMS because as little as 2 hours of LC-MS/MS time
575 will allow to quantify label incorporation for a good number of the more abundant species in a
576 sample. For example, in bioreactors with 63 species we were consistently able to obtain
577 sufficient measurement depth to quantify heavy water incorporation in >=20 species (Fig. 6). In
578 contrast, nanoSIMSonly allows for measurement of isotope incorporation into a limited number
579 of individual cells of very few species (2-3) in this time frame as species assignment of cells
580 depends on species specific probes, and DNA-SIP is limited by the number of samples that fit
581 into the ultracentrifuge rotor (usually six) needed for fine scale separation of heavy and light
582 DNA and the cost associated with sequencing of a great number of individual density gradient
583 fractions per sample. Second, our approach is a departure from previously developed Protein-SIP
584 approaches in that it is highly sensitive and affords a large dynamic range of three orders of
585 magnitude detecting label incorporation in the range of 0.01-10% of added label, while previous
586 Protein-SIP detection principles require much higher label amounts to enable detection and
587 usually offer only a dynamic range of one order of magnitude[21]. Similar is true for DNA/RNA-
588 SIP based approaches, which require at least 20% label for detection[8]. The high sensitivity,
589 accuracy and large dynamic range of our approach brings numerous advantages, including
590 significant cost reduction due to lower use of often very expensive isotopically labeled
591 substrates, the ability to work with much shorter labeling times, and simultaneous detection of
592 label incorporation in slow and fast growing microorganisms. A massive cost reduction
593 compared to other SIP approaches is possible, because most existing (Protein-)SIP approaches
594 use upward of 20% (most often 100%) labeled substrate, while when using the Calis-p approach
595 experiments with 1-10% label can be done cutting the experimental isotope use by 50-99%.
596 Using shorter incubation times is possible because incorporation of labels into proteins does not
597 require for replication to occur, which is the case for DNA-SIP. It is important to note here that
598 the ^{13}C-label content of the substrate needs to be kept at 10% or below for our approach to work
599 (higher percentages can be used for other elements see Box). A short labeling pulse with a
600 substrate with higher label percentage would generate a heavy peptide population that would be
601 completely mass shifted away from the unlabeled peptide population and thus become

602 undetectable by Calis-p. Such strongly mass shifted peptide populations would be detectable
603 with the MetaProSIP[19] and SIPPER[20] softwares. Third, we developed our approach to work
604 with stable isotopes of all elements present in proteins, which allows tracking of assimilation of a
605 large diversity of simple and complex substrates, as well as general activity markers such as ^{18}O
606 water. Based on our ^{2}H and ^{18}O case study results, we would recommend to use ^{18}O water as the
607 activity marker if compatible with the experimental design, as the current Calis-p version showed
608 much higher sensitivity with the 18O data. More testing and optimization of Calis-p will be
609 needed in the future for deuterated water using data to be generated with lower 2H labeling
610 amounts. Fourth, Protein-SIP does not require isotope based separations of biological material
611 such as the density gradient centrifugation used for DNA/RNA-SIP. That approach requires large
612 amounts of material and sequencing of multiple fractions per sample. For this reason, Protein-
613 SIP can be done with very small amounts of sample with an ideal starting amount of 1 mg or
614 more of wet weight cell mass[14]. However, we have achieved good isotope estimates with as
615 little as 50 µg using Calis-p for stable isotope fingerprinting[42].
616 Currently, Protein-SIP only allows for labeling with one isotope per sample as changes in
617 peptide isotope patterns cannot be attributed to specific elements. However, in the future it might
618 be possible to develop Protein-SIP approaches that allow for parallel measurement of ^{15}N and
619 ^{13}C incorporation in a single sample, because added neutron masses for ^{15}N and ^{13}C are
620 sufficiently different from each other - due to differences in nuclear binding energy- to allow for
621 their separation in ultra-high resolution mass spectrometers (Suppl. Results and Discussion). The
622 current limitation for generating ultra-high resolution data suitable for separating peptide carbon
623 and nitrogen isotopes is that higher resolution comes at slower mass spectrometric acquisition
624 time. Thus, there is a tradeoff between ultra-high resolution data acquisition and obtaining a
625 large number of MS^2 spectra for peptide identification. Instruments with faster acquisition times
626 and potentially alternative data acquisition modes such as data-independent acquisition (DIA)
627 metaproteomics could make dual-label Protein-SIP feasible in the next few years.

628 Methods

629 Generation of labeled pure culture samples

630 The following steps were followed for single-carbon labeled and six-carbon labeled ^{13}C glucose
631 experiments with both *Escherichia coli* K12 (Obtained from Salmonella Genetic Stock Centre at
632 the University of Calgary, Catalogue # SGSC 268) and *Bacillus subtilis* strain ATCC 6051. M9
633 and *Bacillus* minimal media were prepared without glucose. For M9 minimal medium we
634 dissolved Na_2HPO_4 (12.8 g), KH_2PO_4 (3.0 g), NaCl (0.5 g), NH_4Cl (1.0 g) in DI Water (978 ml)
635 and autoclaved. Once the solution had cooled, we added the following filter-sterilized solutions:
636 1 M $MgSO_4$ (2 ml), 1 M $CaCl_2$ (0.1 ml), and 0.5% w/v thiamine (0.1 ml). Bacillus minimal
637 medium (0.062 M K_2HPO_4, 0.044 M KH_2PO_4, 0.015 M $(NH_4)_2SO_4$, 0.000 8 M $MgSO_4$ x 7 H_2O)
638 was prepared, the pH adjusted to 7 and autoclaved.

639 20% stock solutions of both unlabeled and ^{13}C-labeled glucose were combined to make a total of
640 eight glucose mixes with final ^{13}C-labeling percentages (% w/w) as follows: 0, 0.01, 0.025, 0.1,
641 0.25, 1, 5, and 10. Please note that the unlabeled glucose contained natural abundances of ^{13}C of
642 around 1.1% and that the percentage of ^{13}C from labeled glucose has to be added to this. For
643 unlabeled glucose we used D-(+)- glucose (> 99.5%) from Sigma Life Science, cat no. G7021
644 and for labeled glucose we used either D-glucose-U-^{13}C (99%, Cambridge Isotope Laboratories,
645 cat no CLM-1396-10) or D-glucose-2-^{13}C glucose (99%, Aldrich, cat no. 310794). **Cell growth**:
646 Frozen stock cultures were streaked on LB agar plates and incubated overnight at 37˚C. A single
647 colony was picked from the plate and grown overnight at 37˚C in liquid media. Nine milliliters
648 of overnight culture were spun down at 18,000 g for five minutes, the supernatant was discarded
649 and pellets were washed twice with PBS to remove unlabeled glucose. Pellets were resuspended
650 in 1 ml PBS. **Labeling**: Ten milliliters of liquid media without glucose were aliquoted into a
651 total of 24 serum bottles per strain (triplicate bottles for each of the eight $^{12}C/^{13}C$ glucose mixes).
652 200 µl of the $^{12}C/^{13}C$ mixes and 10 µl of overnight culture were added into the serum bottles.
653 The bottles were then crimped, the headspace was flushed three times with CO_2-free air and
654 cultures were incubated overnight at 37˚C while shaking at 100 RPM. **Sample processing**:
655 Serum bottles were depressurized by inserting a sterilized needle into the septum to release air.
656 Ten milliliters of culture from each bottle were spun down at 18,000 g for five minutes. The
657 supernatant was discarded and the pellet resuspended in 2 ml of PBS to make two 1 ml aliquots.
658 50 µl of 1%, 5% and 10%-labeled glucose grown cells were used for cell counts using a
659 Neubauer counting chamber. Cells were pelleted at 10,000 g for five minutes, the supernatant
660 was discarded and pellets were flash-frozen in liquid nitrogen before being transferred to -80°C.

661 Mock community spike-in experiments

662 The generation of the mock community (UNEVEN type) is described in Kleiner et al. (2017)[22].
663 We mixed *E. coli* cells grown in 1, 5 and 10% $^{13}C_6$-labeled glucose containing media into three
664 replicate samples of this mock community. We mixed the labeled *E. coli* cells in a 1:1 ratio to
665 unlabeled *E. coli* cells already present in the mock community based on cell counts.

666 Heavy water incubations of a microbial community derived from the human 667 intestinal tract

668 The growth conditions, sample preparation and LC-MS/MS methods for the human intestinal
669 microbiota grown in bioreactors has been described in Starke et al.[11]. Briefly, two bioreactors
670 were inoculated with 63 bacterial strains (six phyla) isolated from a healthy human fecal sample.
671 Bioreactors were fed with two custom media formulations representing different diets - high
672 fiber and a high protein (see table S2 in [11]**).** 2 ml batch cultures were set up using material from
673 the bioreactors and 1 ml of pre-reduced, double strength medium (high fiber or protein), as well
674 as 1 ml of unlabeled, ^{18}O or ^{2}H water was added. After a 12 h incubation at 37 °C in an anaerobic
675 chamber samples were collected by centrifugation. The protein sequence database for

676 identification of peptides from these samples was generated from the Uniprot reference
677 proteomes for the species most closely related to the 63 isolates based on the 16S rRNA
678 information published in Starke et al.[11]. When computing ^{18}O and ^{2}H abundances with Calis-p
679 for these samples we corrected for offset, which can be caused by the natural deviation of the ^{13}C
680 abundance from the standard value as described in the supplementary methods.

681 Sample preparation and One-Dimensional (1D) LC-MS/MS

682 Peptide samples for proteomics were prepared as described by Kleiner et al. (2017)[22] following
683 the filter-aided sample preparation protocol described by Wisniewski et al. (2009)[43]. Peptide
684 concentrations were quantified using a Qubit® Protein Assay Kit (Thermo Fisher Scientific).

685 **1D-LC-MS/MS.** Samples were analyzed by 1D-LC-MS/MS as described in Hinzke et al.
686 (2019)[41]. Replicate samples (e.g. replicate 1 at 1%, 5% and 10%) were run consecutively
687 followed by two wash runs and a blank run to reduce carryover. For 1D-LC-MS/MS, 0.4 µg
688 (pure culture samples) or 2 µg of peptide (mock community-spike in samples) were loaded onto
689 a 5 mm, 300 µm i.d. C18 Acclaim PepMap 100 precolumn (Thermo Fisher Scientific) using an
690 UltiMate 3000 RSLCnano Liquid Chromatograph (Thermo Fisher Scientific). After loading, the
691 precolumn was switched in line with either a 50 cm × 75 µm (pure culture samples) or a 75 cm ×
692 75 µm (mock community – spike in samples) analytical EASY-Spray column packed with
693 PepMap RSLC C_{18}, 2 µm material. The analytical column was connected via an Easy-Spray
694 source to a Q Exactive Plus hybrid quadrupole-Orbitrap mass spectrometer (Thermo Fisher
695 Scientific). Peptides were separated on the analytical column using 140 (pure culture samples) or
696 260 (mock community - spike in) min gradients and mass spectra were acquired in the Orbitrap
697 as described by Petersen et al. (2016). The resolution used on the Q Exactive Plus for MS^1 scans,
698 which provide the isotope pattern information used by Calis-p, was 70,000.

699 Peptide identification and data preparation for Calis-p

700 Briefly, the LC-MS/MS data were used as the input for peptide identification using the database
701 search engine SEQUEST HT implemented in Proteome Discoverer 2.2 (Thermo Scientific).
702 Note, other standard search engines such as Andromeda implemented in MaxQuant[44] can be
703 used as well. We used experiments specific protein sequence databases for the searches and these
704 databases have been submitted along with the LC-MS/MS data sets (see Data Availability).
705 Taxonomic information available for protein sequences in the search database, for example from
706 metagenomic binning and classification, was indicated as a prefix in the accession number (e.g.
707 >TAX_00000) to enable Calis-p to report isotope values for each taxonomic group. The searches
708 were modified to increase peptide identification rates for higher label amounts using customized
709 modifications (see Suppl. Results and Discussion). The peptide spectrum matches (PSMs)
710 produced by the search engine were exported from the search engine either in tabular format or
711 in the open format mzIdentML and provided to Calis-p together with the mass spectrometry raw

712 data in the open mzML format. The mzML files were generated from the raw data using
713 MSConvertGUI via ProteoWizard[45] with the following options set: Output format: mzML,
714 Binary encoding precision: 64-bit, Write index: checked, TPP compatibility: checked, Filter:
715 Peak Picking, Algorithm: Vendor, MS Levels: 1 (The MS/MS scans are not needed for isotope
716 pattern extraction).

717 Once input files and optional parameters are provided Calis-p extracts isotope patterns for all
718 identified peptides using a procedure optimized for Protein-SIP. The isotope patterns are
719 extensively filtered for quality and high quality patterns are used for calculation of peptide
720 isotope content using three different models. The "default" model developed for Protein-SIF, the
721 "neutron abundance" model, which usually works best for Protein-SIP, and the "clumpy" model
722 (see Methods). Calis-p automatically provides output files for all three models for taxa, proteins
723 and peptides in a tabulated format that can subsequently be used in statistical and other data
724 analysis softwares such as R.

725 SIP computation algorithms and computational improvements to increase 726 speed and accuracy of isotopic pattern extraction

727 As a starting point for estimation of stable isotope composition of isotopically labeled samples,
728 we augmented the Calis-p software previously developed for estimation of ^{13}C at natural
729 abundance[14]. For estimating natural ^{13}C abundance the software uses a model that assumes
730 random distribution of ^{13}C atoms in peptides, leading to peptide spectra with predictable isotope
731 patterns. These isotope patterns are modelled in Calis-p with Fast Fourier Transformations
732 (FFT). With labeled samples, the shape of spectra cannot be predicted using FFT, because these
733 spectra become mixtures of spectra associated with labeled and unlabeled peptides. Both the
734 proportion of heavy isotopes in the labeled peptides and the extent of labeling - the relative
735 abundances of labeled versus unlabeled populations of peptides - are unknown in advance. .
736 Therefore, we used the following more general equation to infer the number of neutrons from
737 peptide isotope patterns to implement a "neutron abundance" model:

738 $$\text{Equation 1: } \frac{\sum_{p=1}^{n} p \cdot I_p}{\sum_{p=1}^{n} I_p} = \sum_{e=\{C,H,O,N,S\}} \sum_{n=1}^{4} n \cdot \varphi_{e,n} \cdot a_e$$

739 With, on the left, considering an isotope pattern of size *n* peaks, *p* is the peak number, and *I* is the
740 intensity of peak *p*. On the right, for each isotope, *e* is its element [C,H,O,N,S], *n* the number of
741 additional neutrons, *φ* its abundance (fraction), and *a* the number of atoms of the element in the
742 peptide associated with the spectrum. Table 1 shows the estimates for natural abundances of the
743 isotopes used in calculations.

744

Table 1. Estimates for natural abundances of the isotopes used in calculations based on the IUPAC Technical Report on the Atomic Weights of the Elements [46].

	Isotope				
Element	+0	+1	+2	+3	+4
C	0.9889434148335	0.011056585	0	0	0
N	0.996323567	0.003676433	0	0	0
O	0.997574195	0.00038	0.002045805	0	0
H	0.99988	0.00012	0	0	0
S	0.9493	0.0076	0.0429	0	0.0002

We can rearrange this equation to, for example, calculate the fraction of ^{13}C, assuming all other isotopes are at natural abundance, as follows:

Equation 2: $$\varphi_{e=C,n=1} = \left(\frac{\sum_{p=1}^{n} p \cdot I_p}{\sum_{p=1}^{n} I_p} - \sum_{e=\{H,O,N,S\}} \sum_{n=1}^{4} n \cdot \varphi_{e,n} \cdot a_e \right) \div a_C$$

The second SIP computation algorithm was implemented in Calis-p as the "clumpy label" model. When labeling with substrates that contain multiple isotopically labeled atoms, for example fully labeled $^{13}C_{1\text{-}6}$ glucose, this can lead to assimilation of clumps of labeled atoms into a single amino acid. For example, fully labeled glucose will be converted to fully labeled pyruvate, which, in turn, will be converted to fully labeled alanine, which will be incorporated into protein. This leads to peptide spectra that display higher-than-expected intensity at a higher isotopic peak numbers. To estimate the "clumpiness" of heavy isotopes in peptides, we developed the following procedure (detailed explanation in Figure S6): First, only the monoisotopic peak (A = +0) and A+1 peaks of the spectrum are used to estimate the fraction assimilated in clumps of one heavy atom (e.g. ^{13}C). Next, the experimental intensity of the A+2 peak is compared to its expected intensity assuming all label was assimilated in clumps of one heavy atom. Any additional intensity of the A+2 peak is assigned to assimilation of clumps of two heavy atoms. This way, all peaks up to A+6 are inspected. The algorithm assumes the peptides are completely labeled, i.e. labeled to saturation. Usually, stable isotope probing experiments do not proceed that long, but doing so would enable determination of the number of labeled atoms in the substrate assimilated by each species via this procedure.

768 In typical proteomics data, tens to hundreds of MS1 spectra are collected for each
769 detected peptide, at different elution times and mass over charge ratios. MS1 spectra can be
770 crowded, especially for samples from more complex microbial communities. Unfortunately,
771 overlap between isotopic patterns associated with different peptides can lead to overestimation of
772 labeling. We have added new filtering routines, which remove such compromised isotopic
773 patterns in two steps. First, any isotopic patterns with uneven spacing between peaks (which
774 could indicate overlap with another spectrum) are discarded. On average, the peaks that form an
775 isotopic pattern associated with a given peptide are separated by 1.002 Da, divided by the charge
776 z of the peptide. If a pattern's median peak spacing was <1.000/z or >1.004/z, or if the average
777 sum of squares of the difference between the actual spacings and the median spacing was >
778 1×10-5, the entire isotopic pattern was discarded.

779 Next, remaining spectra are filtered out by unsupervised Markov clustering of all
780 remaining spectra associated with a peptide[47]. The premise of this filtering approach is that
781 clean spectra will be similar to each other, while spectra affected by noise are likely to be more
782 different from each other. After filtering, all remaining spectra are truncated to the most common
783 number of peaks, and spectra with fewer peaks are discarded. Spectra are then normalized to a
784 total intensity of *1*, and an average (weighed by total spectral intensity) normalized spectrum was
785 calculated for each peptide. The averages are weighed by intensity because high intensity spectra
786 are more accurate and less noisy.

787 The normalized spectrum of each peptide is used to estimate the peptide's isotopic
788 composition using the original "Fast Fourier Transformations" based model (also called
789 "default"), as well as the new "neutron abundance" (Equation 1) and "clumpy label" models..
790 For each species and protein in the sample, two center statistics are calculated based on all
791 peptides associated with a species or protein: the median and the intensity-weighted average. The
792 supplementary methods provide a detailed discussion of which center statistic to use when.

793 Generating an additional label incorporation measure and Increasing 794 peptide identification by using mass shift modifications in peptide 795 identification searches

796 In addition to estimates based on MS1 spectra, we also estimated the degree of labeling
797 based on the output of the search engine used for peptide identification. For this, we defined six
798 custom post-translational modifications in the search engine that enable the dynamic addition of
799 1-6 neutrons to a peptide during the search. We tested multiple implementations of these
800 dynamic modifications (Figs. 2 & S2, Suppl. Results & Discussion). Details on the
801 implementation of the modifications in a search engine can be found in the Calis-p software
802 documentation (https://sourceforge.net/p/calis-p/wiki/PSM%20files/).

803 ## Other improvements of the Calis-p software

804 In addition to expanded functionality with regard to filtering of peptides and labeling, the
805 software was also improved in many other ways: It now computes isotopic content of peptides
806 with post-translational modifications and peptides containing sulfur peptides. It finds many more
807 MS1 spectra for each peptide by searching for spectra at additional mass to charge ratios. Next to
808 tab-delimited text PSM files exported from Proteome Discoverer, it now also parses open source
809 mzidentml XML files (http://www.psidev.info/mzidentml). Finally, code efficiency
810 improvements and implementation of multi-threading led to much faster computation, requiring
811 less than one minute to process all spectra recorded during a 2 h run on a QExactive Plus
812 Orbitrap mass spectrometer, using 10 threads. Source code and more details about algorithms
813 and procedures can be found at http://sourceforge.net/projects/calis-p/.

814 ## Comparison with existing Protein-SIP tools

815 To benchmark and compare Calis-p against existing Protein-SIP tools under optimal
816 operation conditions, we invited developers/operators of Sipros [17], MetaProSIP [19] and SIPPER
817 [20] to participate in a tool comparison. Drs. Sachsenberg (MetaProSIP) and Tolić (SIPPER)
818 joined our effort. We were unfortunately not able to find an operator for Sipros and were also
819 unable to get the tool to work on our own. For the comparison we used four raw files from the
820 mock community spike-in experiments including unlabeled, 1% label, 5%, label, and 10% label
821 in the spiked in *E. coli* and the corresponding protein sequence database. For processing with
822 Calis-p we used the optimized settings from this study.

823 The SIPPER tool was developed at the Pacific Northwest National Laboratory and is
824 available as an open source software written in C#. SIPPER requires an unlabeled incubation MS
825 dataset as a reference for extracting target peptide IDs to which all stable isotope incubated
826 datasets are compared. To generate peptide-spectrum matches to be used for isotope estimates
827 the MSGF+ search algorithm [48] was used to search the unlabeled sample against the protein
828 sequence database. The precursor mass tolerance was set to 20 ppm and oxidation of M and N-
829 terminal acetylation were included as dynamic modifications and carbamidomethylation of C as
830 static modification –, The search provided 112,580 identified target sequences (including
831 contaminant IDs). The parameters for the SIPPER isotope calculation run included summing 7
832 precursor spectra around each target scan number, a 10 ppm tolerance for mass accuracy, 10%
833 tolerance for normalized elution time, and filter confidence ID criteria outlined in the
834 manuscript.

835 The MetaProSIP tool is integrated into the OpenMS open source software GUI[49]. An
836 OpenMS workflow including a database search with Comet followed by the MetaProSIP tool
837 was built according to the recommended parameters from the original publication with the minor
838 modification that we activated the MetaProSIP setting to subtract the mono isotopic peak value.

839 A reference (unlabeled) incubation was not needed to perform isotope calculations, because we
840 expected part of the *E. coli* peptide population in the sample to be unlabeled due to the presence
841 of unlabeled E. coli in the mock community thus all four data files were run through the
842 workflow. The database search parameters were 10 ppm mass tolerance for precursor ions, up to
843 two missed cleavages, carbamidomethylation of C as static modification, and oxidation of M as
844 dynamic modification. Results were reported as relative isotope abundances (RIA) per ID. The
845 MetaProSIP algorithm can split the RIA distributions of peptides with higher abundances into
846 multiple isotope abundance clusters, leading to multiple reported RIAs per peptide. This
847 happened on average for ~9% of peptides in our datasets (0.3% in unlabeled, 6% in 1% labeled,
848 14% in 5% labeled, and 13% in 10% labeled). If the algorithm provided multiple RIAs for a
849 peptide, we only used the highest RIA value in all downstream calculations.

850 To make the output data from both SIPPER and MetaProSIP comparable to the Calis-p
851 output we used the tables from both approaches that report 13C content per PSM or peptide.
852 SIPPER 13C content was reported in terms of percent carbon and percent peptides labeled,
853 MetaProSIP 13C content was reported as relative isotope abundance, and Calis-p $^{13}C/^{12}C$ ratios
854 were converted to 13C atom percent. We filtered the data to only include distinct protein unique
855 peptides then calculated the 13C content for each species by taking the median. For visual
856 representations (Fig. S4), we additionally filtered the data for which 13C values were provided
857 for at least 9 peptides per species (equivalent to filter used for Calis-p).

858 **Data and software availability**

859 The Calis-p (version 2.1) was implemented in Java and is freely available for download, use and
860 modification at http://sourceforge.net/projects/calis-p/ and with a stable identifier at Zenodo
861 https://doi.org/10.5281/zenodo.5619585 (Reviewer access can be obtained via this link
862 https://datadryad.org/stash/share/HYoUsJAbcrkBaoPumrts4rcxSTMHO1iifjL-5YE3SU0).

863

864 The MS proteomics data and the protein sequence databases have been deposited to the
865 ProteomeXchange Consortium [50] via the PRIDE partner repository with the following dataset
866 identifiers: *B. subtilis* and *E. coli* grown in minimal medium with fully labeled $^{13}C_{1-6}$-glucose at
867 different concentrations PXD023693 [Reviewer Access at: https://www.ebi.ac.uk/pride/login
868 User: reviewer_pxd023693@ebi.ac.uk Password: 0AyI3dGY], *B. subtilis* and *E. coli* grown in
869 minimal medium with singly labeled $^{13}C_2$-glucose at different concentrations PXD024285
870 [Reviewer Access at: https://www.ebi.ac.uk/pride/login User: reviewer_pxd024285@ebi.ac.uk
871 Password: 0oSaTgAW], labeled E. coli spiked into the mock community PXD024174
872 [Reviewer Access at: https://www.ebi.ac.uk/pride/login User: reviewer_pxd024174@ebi.ac.uk
873 Password: axKUZrEV], mixing of labeled and unlabeled *E. coli* PXD024287 [Reviewer Access
874 at: https://www.ebi.ac.uk/pride/login User: reviewer_pxd024287@ebi.ac.uk Password:

875 VmwP04XB], *E. coli* labeled to saturation with 2.5% ^{15}N ammonium PXD024288 [Reviewer
876 Access at: https://www.ebi.ac.uk/pride/login User: reviewer_pxd024288@ebi.ac.uk Password:
877 oQcd2WjH], and the human microbiota derived microbial community from Starke et al. [11]
878 grown with heavy water and different diets PXD024291 [Reviewer Access at:
879 https://www.ebi.ac.uk/pride/login User: reviewer_pxd024291@ebi.ac.uk Password: GHbI87wI].

880 The mock community data without labeled *E. coli* spike-in was previously published [22]
881 and we retrieved files Run4_U2_4600ng.msf and Run5_U2_4600ng.msf from PRIDE Project
882 PXD006118.

883 Author contributions

884 M.K. and M.S. designed research; M.K., A.Kouris., J.M., and M.S. performed research; M.K.,
885 A.Kouris., M.J., Y.L., A.Korenek, G.D., T.S., N.T., M.L., and M.S. analyzed data; and M.K.
886 and M.S. wrote the paper with support from all co-authors.

887 Acknowledgements

888 We thank Nico Jehmlich and Robert Starke for providing the raw data for the heavy water
889 dataset, and J. Alfredo Blakely-Ruiz for comments on the manuscript.

890 This work was supported by USDA National Institute of Food and Agriculture Hatch project
891 1014212 (MK), by the National Institute Of General Medical Sciences of the National Institutes
892 of Health under Award Number R35GM138362 (MK), the U.S. National Science Foundation
893 grant OIA #1934844, the Novo Nordisk Foundation INTERACT project under Grant number
894 NNF19SA0059360 (MK), the Foundation for Food and Agriculture Research Grant ID: 593607
895 (MK), the Canada Foundation for Innovation (#32181, MS), the Natural Sciences and
896 Engineering Research Council (NSERC), the Canada First Research Excellence Fund (CFREF),
897 the Government of Alberta, and the University of Calgary.

898 Competing interests

899 The authors have no competing interests to declare.

900 References

901 1. Kleiner M, Wentrup C, Holler T, Lavik G, Harder J, Lott C, et al. Use of carbon monoxide
902 and hydrogen by a bacteria–animal symbiosis from seagrass sediments. Environ Microbiol
903 2015;17(12):5023–35.
904 2. Mayali X. NanoSIMS: Microscale Quantification of Biogeochemical Activity with Large-
905 Scale Impacts. Annu Rev Mar Sci 2020;12(1):449–67.

3. Berry D, Loy A. Stable-Isotope Probing of Human and Animal Microbiome Function. Trends Microbiol 2018;26(12):999–1007.
4. Kong Y, Kuzyakov Y, Ruan Y, Zhang J, Wang T, Wang M, et al. DNA Stable-Isotope Probing Delineates Carbon Flows from Rice Residues into Soil Microbial Communities Depending on Fertilization. Appl Environ Microbiol [Internet] 2020 [cited 2021 Mar 4];86(7). Available from: https://aem.asm.org/content/86/7/e02151-19
5. Pett-Ridge J, Firestone MK. Using stable isotopes to explore root-microbe-mineral interactions in soil. Rhizosphere 2017;3:244–53.
6. Hatzenpichler R, Scheller S, Tavormina PL, Babin BM, Tirrell DA, Orphan VJ. In situ visualization of newly synthesized proteins in environmental microbes using amino acid tagging and click chemistry. Environ Microbiol 2014;16(8):2568–90.
7. Hatzenpichler R, Krukenberg V, Spietz RL, Jay ZJ. Next-generation physiology approaches to study microbiome function at single cell level. Nat Rev Microbiol 2020;18(4):241–56.
8. Radajewski S, Ineson P, Parekh NR, Murrell JC. Stable-isotope probing as a tool in microbial ecology. Nature 2000;403(6770):646–9.
9. Jehmlich N, Vogt C, Lünsmann V, Richnow HH, von Bergen M. Protein-SIP in environmental studies. Curr Opin Biotechnol 2016;41:26–33.
10. Justice NB, Li Z, Wang Y, Spaudling SE, Mosier AC, Hettich RL, et al. 15N- and 2H proteomic stable isotope probing links nitrogen flow to archaeal heterotrophic activity. Environ Microbiol 2014;16(10):3224–37.
11. Starke R, Oliphant K, Jehmlich N, Schäpe SS, Sachsenberg T, Kohlbacher O, et al. Tracing incorporation of heavy water into proteins for species-specific metabolic activity in complex communities. J Proteomics 2020;222:103791.
12. Eichorst SA, Strasser F, Woyke T, Schintlmeister A, Wagner M, Woebken D. Advancements in the application of NanoSIMS and Raman microspectroscopy to investigate the activity of microbial cells in soils. FEMS Microbiol Ecol [Internet] 2015 [cited 2021 Mar 8];91(fiv106). Available from: https://doi.org/10.1093/femsec/fiv106
13. Musat N, Musat F, Weber PK, Pett-Ridge J. Tracking microbial interactions with NanoSIMS. Curr Opin Biotechnol 2016;41:114–21.
14. Kleiner M, Dong X, Hinzke T, Wippler J, Thorson E, Mayer B, et al. Metaproteomics method to determine carbon sources and assimilation pathways of species in microbial communities. Proc Natl Acad Sci U S A 2018;115(24):E5576–84.
15. Mann M. Fifteen Years of Stable Isotope Labeling by Amino Acids in Cell Culture (SILAC) [Internet]. In: Warscheid B, editor. Stable Isotope Labeling by Amino Acids in Cell Culture (SILAC): Methods and Protocols. New York, NY: Springer; 2014 [cited 2020 Nov 12]. page 1–7.Available from: https://doi.org/10.1007/978-1-4939-1142-4_1
16. Kleiner M. Metaproteomics: Much More than Measuring Gene Expression in Microbial Communities. mSystems 2019;4(3):e00115-19.
17. Pan C, Fischer CR, Hyatt D, Bowen BP, Hettich RL, Banfield JF. Quantitative tracking of isotope flows in proteomes of microbial communities. Mol Cell Proteomics 2011;10(4).
18. Marlow JJ, Skennerton CT, Li Z, Chourey K, Hettich RL, Pan C, et al. Proteomic Stable Isotope Probing Reveals Biosynthesis Dynamics of Slow Growing Methane Based Microbial Communities. Front Microbiol [Internet] 2016 [cited 2019 Sep 26];7. Available from: https://www.frontiersin.org/articles/10.3389/fmicb.2016.00563/full
19. Sachsenberg T, Herbst FA, Taubert M, Kermer R, Jehmlich N, von Bergen M, et al. MetaProSIP: Automated Inference of Stable Isotope Incorporation Rates in Proteins for

952 Functional Metaproteomics. J Proteome Res 2015;14(2):619–27.
953 20. Slysz GW, Steinke L, Ward DM, Klatt CG, Clauss TRW, Purvine SO, et al. Automated
954 Data Extraction from In Situ Protein-Stable Isotope Probing Studies. J Proteome Res
955 2014;13(3):1200–10.
956 21. Starke R. Quantification of the necessary labelling input in protein stable isotope probing.
957 bioRxiv 2020;2020.06.02.129254.
958 22. Kleiner M, Thorson E, Sharp CE, Dong X, Liu D, Li C, et al. Assessing species biomass
959 contributions in microbial communities via metaproteomics. Nat Commun 2017;2017:1558.
960 23. Berry D, Mader E, Lee TK, Woebken D, Wang Y, Zhu D, et al. Tracking heavy water
961 (D2O) incorporation for identifying and sorting active microbial cells. Proc Natl Acad Sci
962 2015;112(2):E194–203.
963 24. Zhang R, Sioma CS, Wang S, Regnier FE. Fractionation of isotopically labeled peptides in
964 quantitative proteomics. Anal Chem 2001;73(21):5142–9.
965 25. Zhang R, Sioma CS, Thompson RA, Xiong L, Regnier FE. Controlling deuterium isotope
966 effects in comparative proteomics. Anal Chem 2002;74(15):3662–9.
967 26. Hayes JM. Fractionation of carbon and hydrogen isotopes in biosynthetic processes. Rev
968 Mineral Geochem 2001;43(1):225–77.
969 27. Englander SW, Sosnick TR, Englander JJ, Mayne L. Mechanisms and uses of hydrogen
970 exchange. Curr Opin Struct Biol 1996;6(1):18–23.
971 28. Taubert M, Stöckel S, Geesink P, Girnus S, Jehmlich N, von Bergen M, et al. Tracking
972 active groundwater microbes with D2O labelling to understand their ecosystem function.
973 Environ Microbiol 2018;20(1):369–84.
974 29. Lovett S. Effect of Deuterium on Starving Bacteria. Nature 1964;203(4943):429–30.
975 30. Schnölzer M, Jedrzejewski P, Lehmann WD. Protease-catalyzed incorporation of 18O into
976 peptide fragments and its application for protein sequencing by electrospray and matrix-
977 assisted laser desorption/ionization mass spectrometry. ELECTROPHORESIS
978 1996;17(5):945–53.
979 31. Reese AT, Pereira FC, Schintlmeister A, Berry D, Wagner M, Hale LP, et al. Microbial
980 nitrogen limitation in the mammalian large intestine. Nat Microbiol 2018;3(12):1441.
981 32. Holmes AJ, Chew YV, Colakoglu F, Cliff JB, Klaassens E, Read MN, et al. Diet-
982 Microbiome Interactions in Health Are Controlled by Intestinal Nitrogen Source
983 Constraints. Cell Metab 2017;25(1):140–51.
984 33. Chijiiwa R, Hosokawa M, Kogawa M, Nishikawa Y, Ide K, Sakanashi C, et al. Single-cell
985 genomics of uncultured bacteria reveals dietary fiber responders in the mouse gut
986 microbiota. Microbiome 2020;8(1):5.
987 34. Patnode ML, Beller ZW, Han ND, Cheng J, Peters SL, Terrapon N, et al. Interspecies
988 Competition Impacts Targeted Manipulation of Human Gut Bacteria by Fiber-Derived
989 Glycans. Cell 2019;179(1):59-73.e13.
990 35. Desai MS, Seekatz AM, Koropatkin NM, Kamada N, Hickey CA, Wolter M, et al. A
991 dietary fiber-deprived gut microbiota degrades the colonic mucus barrier and enhances
992 pathogen susceptibility. Cell 2016;167(5):1339-1353.e21.
993 36. Sanders ME, Merenstein DJ, Reid G, Gibson GR, Rastall RA. Probiotics and prebiotics in
994 intestinal health and disease: from biology to the clinic. Nat Rev Gastroenterol Hepatol
995 2019;16(10):605–16.
996 37. Poeker SA, Geirnaert A, Berchtold L, Greppi A, Krych L, Steinert RE, et al. Understanding
997 the prebiotic potential of different dietary fibers using an in vitro continuous adult

998 fermentation model (PolyFermS). Sci Rep 2018;8(1):4318.
999 38. Smyth P, Zhang X, Ning Z, Mayne J, Moore JI, Walker K, et al. Studying the Temporal
1000 Dynamics of the Gut Microbiota Using Metabolic Stable Isotope Labeling and
1001 Metaproteomics. Anal Chem [Internet] 2020 [cited 2021 Mar 17];Available from:
1002 https://pubs.acs.org/doi/pdf/10.1021/acs.analchem.0c02070
1003 39. Mayers MD, Moon C, Stupp GS, Su AI, Wolan DW. Quantitative metaproteomics and
1004 activity-based probe enrichment reveals significant alterations in protein expression from a
1005 mouse model of inflammatory bowel disease. J Proteome Res 2017;16(2):1014–26.
1006 40. Li Z, Yao Q, Guo X, Crits-Christoph A, Mayes MA, Iv WJH, et al. Genome-Resolved
1007 Proteomic Stable Isotope Probing of Soil Microbial Communities Using 13CO2 and 13C-
1008 Methanol. Front Microbiol 2019;10:2706.
1009 41. Hinzke T, Kouris A, Hughes RA, Strous M, Kleiner M. More is not always better:
1010 Evaluation of 1D and 2D-LC-MS/MS methods for metaproteomics. Front Microbiol
1011 2019;10(238).
1012 42. Seah BKB, Antony CP, Huettel B, Zarzycki J, Borzyskowski LS von, Erb TJ, et al. Sulfur-
1013 Oxidizing Symbionts without Canonical Genes for Autotrophic CO2 Fixation. mBio
1014 2019;10(3):e01112-19.
1015 43. Wiśniewski JR, Zougman A, Nagaraj N, Mann M. Universal sample preparation method for
1016 proteome analysis. Nat Methods 2009;6(5):359–62.
1017 44. Cox J, Neuhauser N, Michalski A, Scheltema RA, Olsen JV, Mann M. Andromeda: a
1018 peptide search engine integrated into the MaxQuant environment. J Proteome Res 2011;10.
1019 45. Chambers MC, Maclean B, Burke R, Amodei D, Ruderman DL, Neumann S, et al. A cross-
1020 platform toolkit for mass spectrometry and proteomics. Nat Biotechnol 2012;30:918–20.
1021 46. Laeter JR de, Böhlke JK, Bièvre PD, Hidaka H, Peiser HS, Rosman KJR, et al. Atomic
1022 weights of the elements. Review 2000 (IUPAC Technical Report). Pure Appl Chem
1023 2003;75(6):683–800.
1024 47. Enright AJ, Van Dongen S, Ouzounis CA. An efficient algorithm for large-scale detection
1025 of protein families. Nucleic Acids Res 2002;30(7):1575–84.
1026 48. Kim S, Pevzner PA. MS-GF+ makes progress towards a universal database search tool for
1027 proteomics. Nat Commun 2014;5(1):5277.
1028 49. Röst HL, Sachsenberg T, Aiche S, Bielow C, Weisser H, Aicheler F, et al. OpenMS: a
1029 flexible open-source software platform for mass spectrometry data analysis. Nat Methods
1030 2016;13(9):741–8.
1031 50. Vizcaino JA, Deutsch EW, Wang R, Csordas A, Reisinger F, Rios D, et al.
1032 ProteomeXchange provides globally coordinated proteomics data submission and
1033 dissemination. Nat Biotechnol 2014;32(3):223–6.

1034

1035

1036